

Supporting Information - Discovery of Small-Molecule Antagonists of the PWWP Domain of NSD2 - Supporting Information

Renato Ferreira de Freitas^{‡,·,·,#}, Yanli Liu^{‡,·,·,#}, Magdalena M. Szewczyk[‡], Naimee Mehta[†], Fengling Li[‡], David McLeod^{††}, Carlos Zepeda-Velázquez^{††}, David Dilworth[‡], Ronan P. Hanley[†], Elisa Gibson[‡], Peter J. Brown[‡], Rima Al-Awar^{††}, Lindsey I. James[†], Cheryl H. Arrowsmith^{‡,&}, Dalia Barsyte-Lovejoy^{‡,!}, Jinrong Min^{‡,%}, Masoud Vedadi^{‡,!}, Matthieu Schapira^{‡,!,*}, Abdellah Allali-Hassani^{‡,·,·,·,#,*}

[‡] Structural Genomics Consortium, University of Toronto, Toronto, Ontario M5G 1L7, Canada

[†] Center for Integrative Chemical Biology and Drug Discovery, Division of Chemical Biology and Medicinal Chemistry, UNC Eshelman School of Pharmacy, University of North Carolina at Chapel Hill, Chapel Hill, North Carolina 27599, United States

^{††} Drug Discovery Program, Ontario Institute for Cancer Research, Toronto, ON M5G 0A3, Canada

[&] Princess Margaret Cancer Centre and Department of Medical Biophysics, University of Toronto, Toronto, ON, M5G 2M9, Canada

[%] Department of Physiology, University of Toronto, Toronto, ON M5S 1A8, Canada

[!] Department of Pharmacology & Toxicology, University of Toronto, Toronto, Ontario M5S 1A8, Canada

[|] present address: Centro de Ciências Naturais e Humanas, Universidade Federal do ABC, Rua Arcturus 3, São Bernardo do Campo, SP 09606-070, Brazil.

^{||} present address: College of Pharmaceutical Sciences, Soochow University, Suzhou, Jiangsu 215123, China

^{|||} present address: Incyte, 1801 Augustine Cut-Off, Wilmington, DE 19803, USA

[#] equal contributors

^{*} To whom correspondence should be addressed

p2: Figure S1

p2: Table S2

p3: Characterization of Compound 1

p3: Figure S2

p3: Figure S3

p4: Figure S4

p5: Figure S5

p6: Figure S6

p6: Table S3

p7: Figure S7

p7: Figure S8

p8: Figure S9

p9-13: ¹H NMR Spectra compounds 3c, 3d.

p14-32: Compound purity: analytical spectra

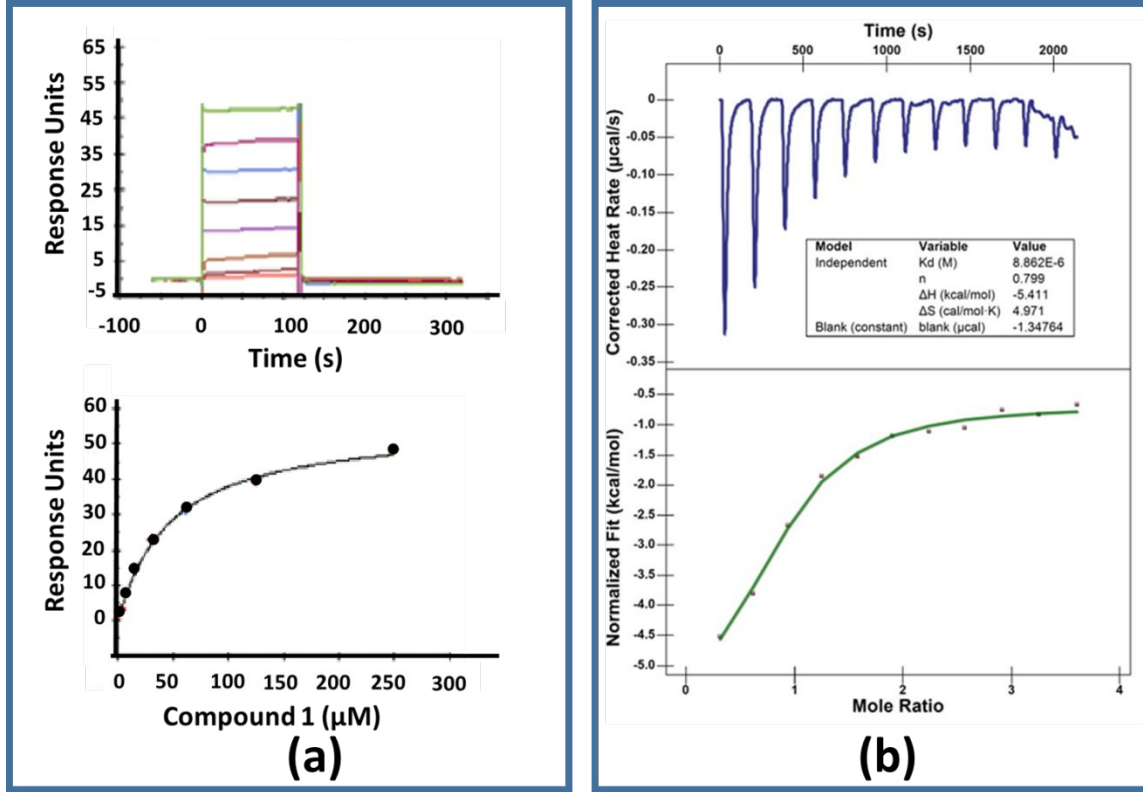


Figure S1. (a) Compound **1** binds NSD2-PWWP1 with a K_d of $41 \pm 8 \mu\text{M}$ in SPR experiments conducted in triplicate. SPR-sensorgram (upper pane) for the interaction of **1** with NSD2-PWWP1 domain. Multi-cycle kinetics was used with concentrations from $2 \mu\text{M}$ to $250 \mu\text{M}$ (dilution factor of 0.5 was used to yield 8 concentrations). 90 s contact time and 120 s dissociation time at $100 \mu\text{L}/\text{min}$ were used. The steady state values were determined and plotted as a function of the concentration (lower pane). A single binding site model was fitted to the data to calculate K_d . (b) ITC results showing raw data after integration baseline correction (upper pane) and integrated data and regression (lower pane). n is the number of molecules per binding site, K_d is the association constant, ΔH is the change in enthalpy, and ΔS is the change in entropy.

Table S2. Thermal shift in differential static light scattering (DSLS) induced by **1** against seven PWWP domains.

Protein	ΔT_{agg} at 400 μM ($^{\circ}\text{C}$)
BRPF1-PWWP	-0.5
DNMT3b-PWWP	-1.2
MSH6-PWWP	-1.4
NSD2-PWWP1	3.9
NSD3-PWWP1	-0.3
ZMYND11-PWWP	-1.2
ZCWPW1-PWWP	-1.4

Characterization of Compound **1**

The original sample was obtained from Enamine (Catalog Number Z1483746373) and assumed to be a racemic mixture. Attempted separation of all 4 diastereoisomers by chiral SFC resulted in only two

peaks in the SFC chromatogram. Peaks showed identical NMR spectra but exhibited equal and opposite optical rotations. These must be enantiomers and thus the original sample must have been made by a diastereoselective route (Figure S2).

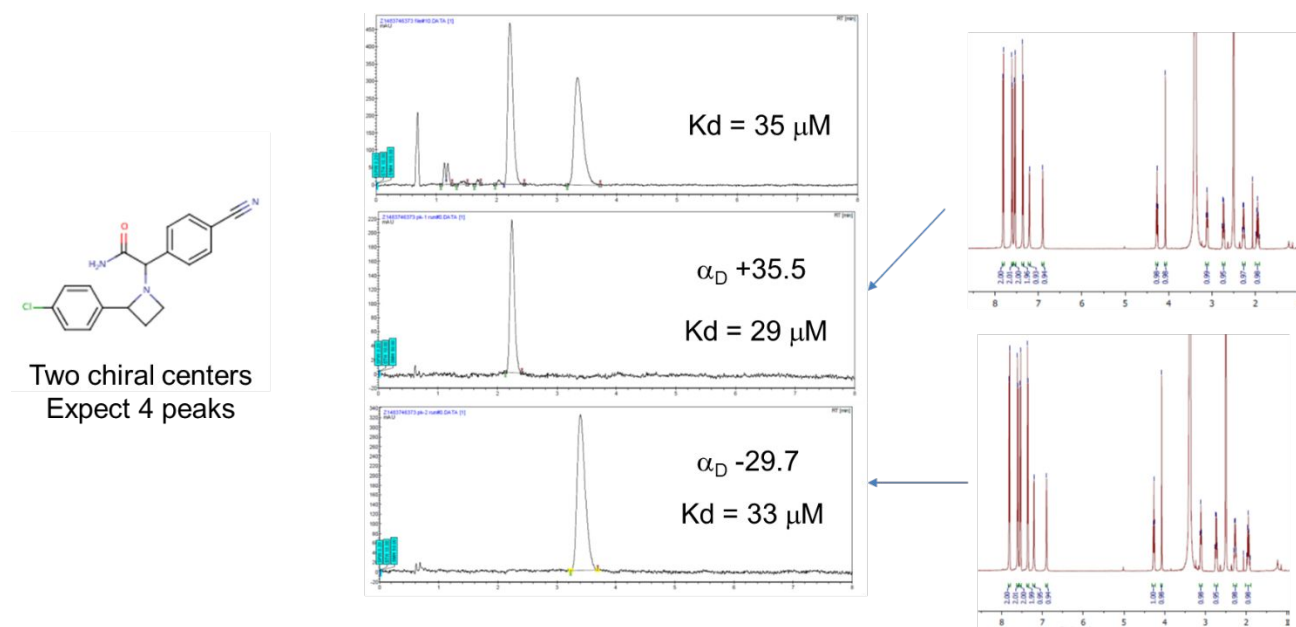


Figure S2. Separation of enantiomers from original sample by chiral SFC.

A search of the literature found a paper describing this diastereoselective synthesis from a substituted boronic acid and cyclic amine (Nanda K. K. and Trotter B. W. *Tet. Lett.* (2005) 2025-28). In an effort to determine the activity of the other diastereoisomers, a non-diastereoselective route was developed involving azetidine displacement of an α -bromoester (Figure S3).

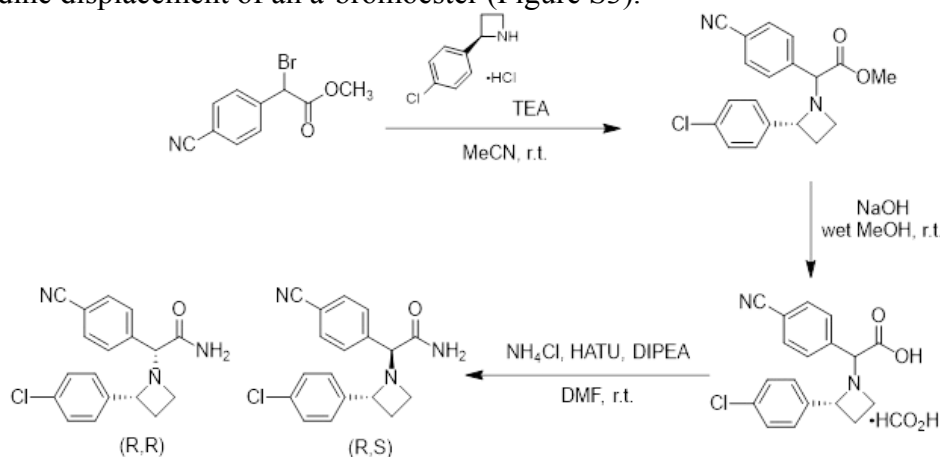


Figure S3. Synthesis from (*R*)-azetidine gave two diastereoisomers. Similar results were obtained starting from (*S*)-azetidine to give the (*S,S*) and (*S,R*) diastereoisomers.

In this case, all four isomers were detected by chiral SFC, however, the diastereoisomers not found in the original material were inactive. The assignment of stereochemistry was based on the diastereoselective product in the original paper which was confirmed by X-ray crystallography (Figure S4).

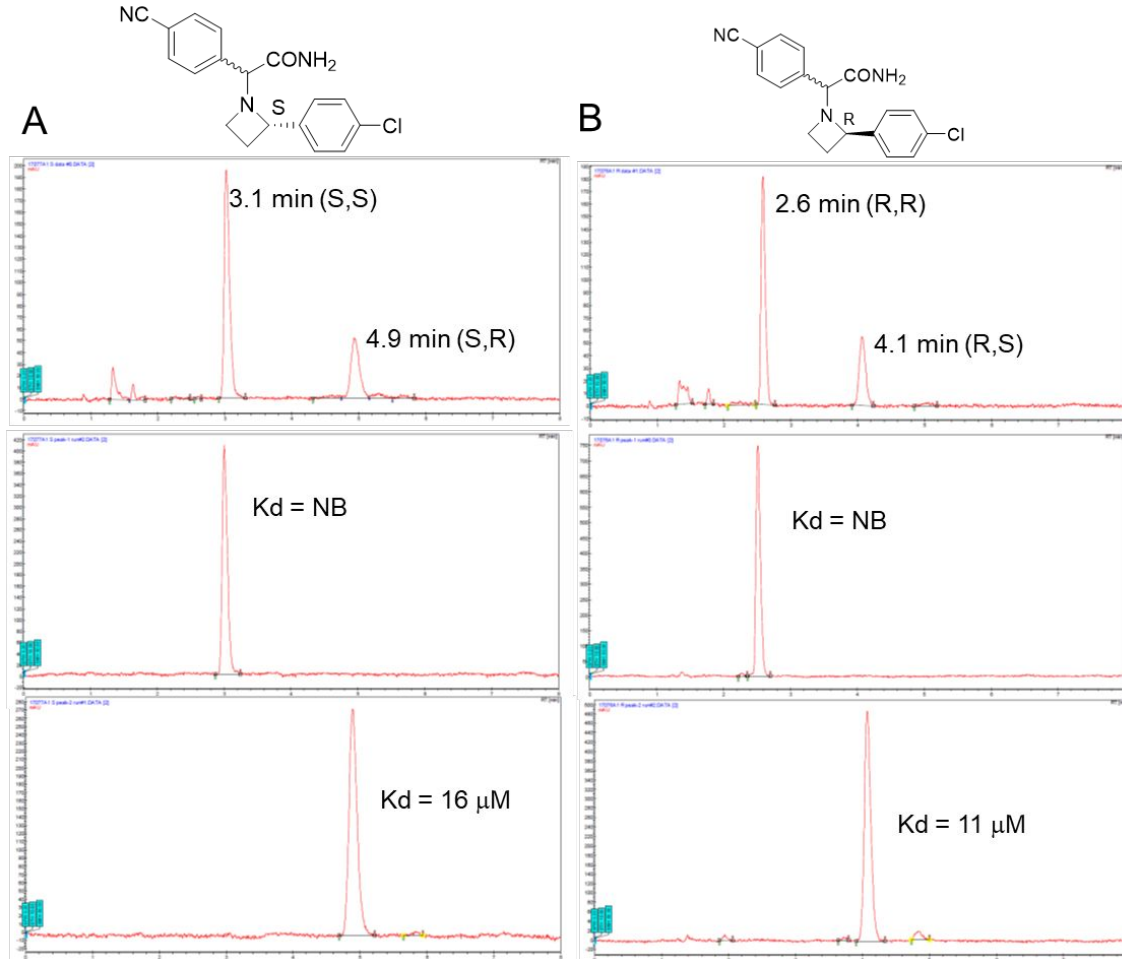


Figure S4. Chiral preparative SFC separation of diastereoisomers. A) Reaction products from (*S*)-azetidine gave peaks at 3.1 and 4.9 mins. B) Products from (*R*)-azetidine gave peaks at 2.6 and 4.1 mins. The original enantiomers correspond to the peaks at 4.1 and 4.9 mins. Lower panels indicate the analytical chiral SFC analysis of collected peaks.

Experimental Procedures and Characterization data

Separation of commercial material

The commercially available material (30 mg; Enamine Z1483746373) was separated by chiral SFC using an IA column (2 x 25 cm) using 30% MeOH/CO₂ as eluant at a flowrate of 60 mL.min⁻¹ and 100 bar pressure. Detection by UV at 220 nm. Injection volume was 1.5 mL of 3 mg.mL⁻¹ in MeOH. Analytical chiral SFC (Fig. 1) used IA column (0.46 x 25 cm) with 40% MeOH/CO₂ as eluant at a flowrate of 3 mL.min⁻¹ and 100 bar pressure. Detection by UV at 220 nm.

2R-(2-(4-chlorophenyl)azetididin-1-yl)-2S-(4-cyanophenyl)acetamide (13 mg). $[\alpha]_d^{23} +35.5^\circ$ (c=0.205; MeOH). ¹H NMR (500 MHz, DMSO) δ 7.81 (d, *J* = 8.2 Hz, 2H), 7.60 (d, *J* = 8.2 Hz, 2H), 7.54 (d, *J* = 8.4 Hz, 2H), 7.36 (d, *J* = 8.4 Hz, 2H), 7.21 (s, 1H), 6.90 (s, 1H), 4.27 (t, *J* = 8.1 Hz, 1H), 4.07 (s, 1H), 3.11 (t, *J* = 6.5 Hz, 1H), 2.73 (dd, *J* = 16.1, 8.0 Hz, 1H), 2.27 (q, *J* = 8.0 Hz, 1H), 1.95 (p, *J* = 9.0 Hz, 1H).

2S-(2-(4-chlorophenyl)azetididin-1-yl)-2R-(4-cyanophenyl)acetamide (12 mg). $[\alpha]_d^{23} -29.7^\circ$ (c=0.337; MeOH). ¹H NMR (500 MHz, DMSO) δ 7.81 (d, *J* = 8.2 Hz, 2H), 7.60 (d, *J* = 8.2 Hz, 2H), 7.54 (d, *J* = 8.3 Hz, 2H), 7.36 (d, *J* = 8.3 Hz, 2H), 7.21 (s, 1H), 6.90 (s, 1H), 4.27 (t, *J* = 8.1 Hz, 1H), 4.07 (s, 1H), 3.11 (t, *J* = 6.5 Hz, 1H), 2.73 (dd, *J* = 16.1, 8.0 Hz, 1H), 2.27 (q, *J* = 8.0 Hz, 1H), 1.95 (p, *J* = 9.0 Hz, 1H).

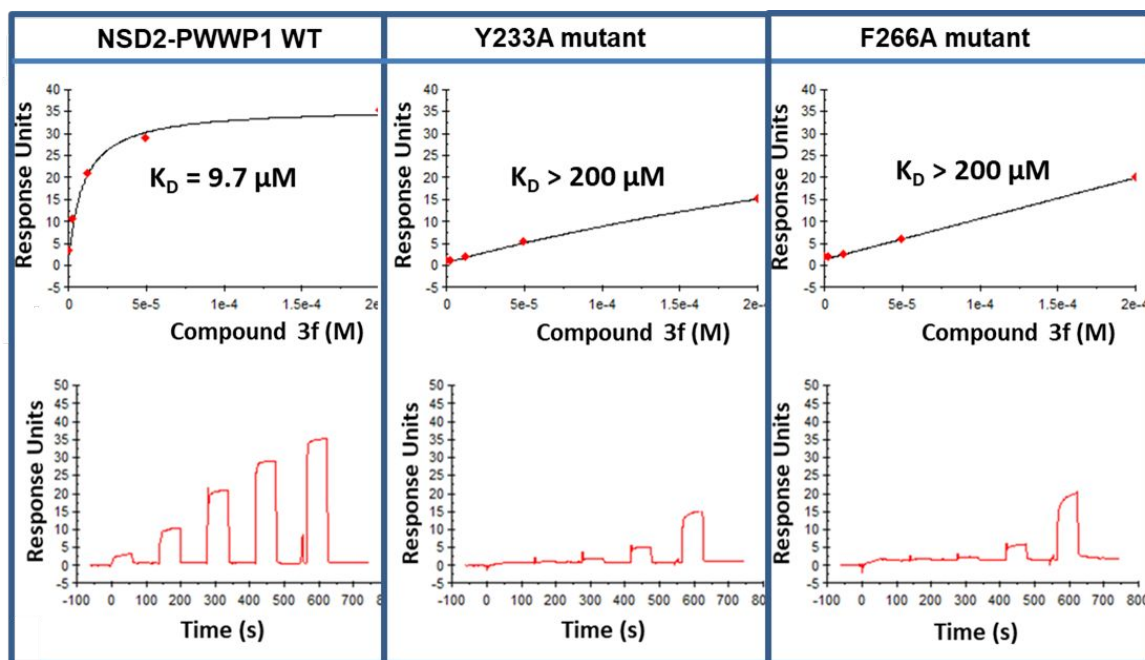


Figure S5: compound **3f** binds wild-type NSD2-PWWP1 but not Y233A or F266A mutants in SPR experiments

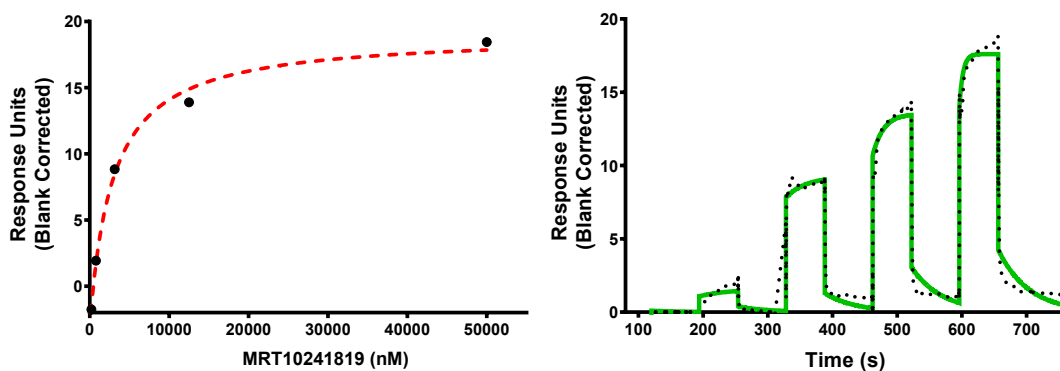


Figure S6. Compound **3f** binds NSD2-PWWP1 with a K_d of $3.42 \pm 0.45 \mu\text{M}$ in a SPR experiments conducted in triplicate with 0.5% DMSO concentration. Biotinylated NSD2-PWWP1 domain (208-368) was immobilized on the flow cell of an SA sensor chip in 1x HBS-EP buffer, yielding 5000 RU. The biotinylated RBBP5 (2-538) was immobilized on another flow cell of SA chip, yielding 4300 RU as a negative control. Using the same buffer with 0.5% DMSO and single cycle kinetics with 60 s contact time and a dissociation time of 120s at a flow rate of $75 \mu\text{L}/\text{min}$. The compound was tested at $50 \mu\text{M}$ as the highest concentration and dilution factor of 0.25 was used to yield 5 concentrations.

Table S3. Crystallography data and refinement statistics

	NSD2 + 3f
PDB Code	6UE6
Data collection	
Space group	$P2_12_12_1$

Cell dimensions	
<i>a</i> , <i>b</i> , <i>c</i> (Å)	69.2, 70.3, 228.8
α , β , γ (°)	90.0, 90.0, 90.0
Resolution (Å)	49.33-2.40(2.49-2.40)
(highest resolution shell)	
Measured reflections	287140
Unique reflections	44525
<i>R</i> _{merge}	8.4(0.997)
<i>I</i> / σ <i>I</i>	14.0(1.9)
Completeness(%)	99.7(97.5)
Redundancy	6.4(5.2)
Refinement	
Resolution (Å)	45.3-2.40
No. reflections (test set)	44447(2275)
<i>R</i> _{work} / <i>R</i> _{free} (%)	23.6/25.2
No. atoms	
Protein	7136
Compound	160
B-factors (Å ²)	
Protein	61.4
Compound	47.5
RMSD	
Bond lengths (Å)	0.010
Bond angles (°)	0.99
Ramachandran plot % residues	
Favored	99.5
Additional allowed	0.5
Generously allowed	0
Disallowed	0

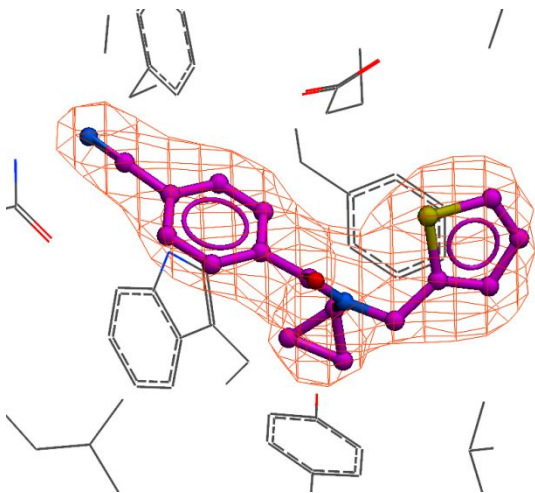
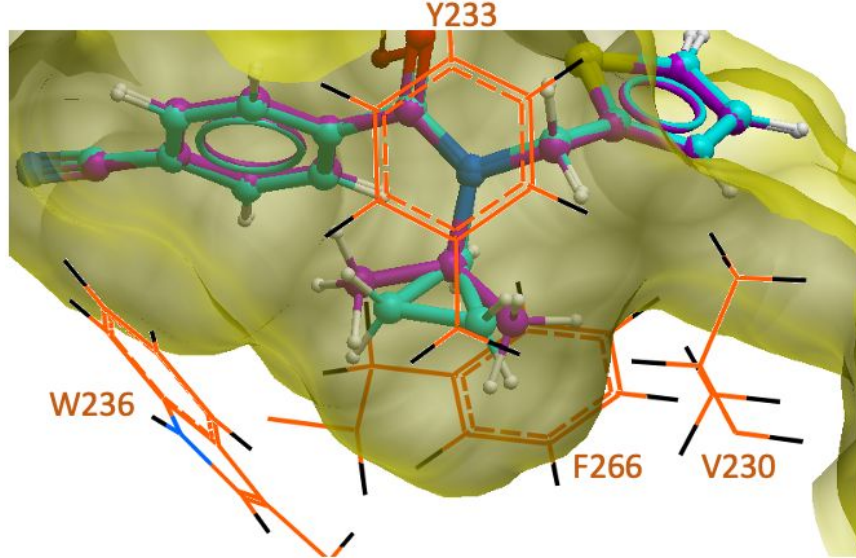


Figure S7: One sigma electron density unambiguously defines the ligand binding pose

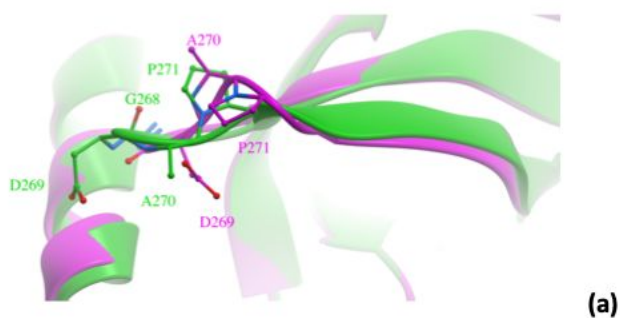


Ligand interaction VdW Energy

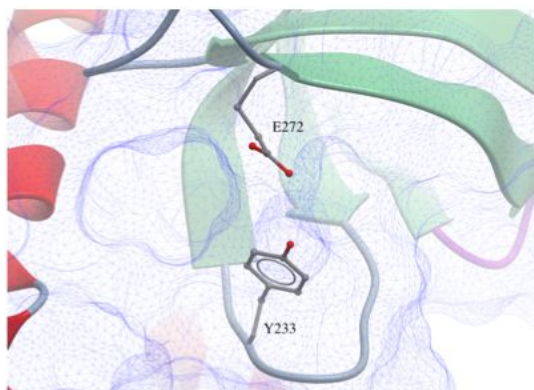
compound **3f** (cyclopropyl) : -27.5 kcal/mol

Compound **3c** (isopropyl): 1.1 kcal/mol

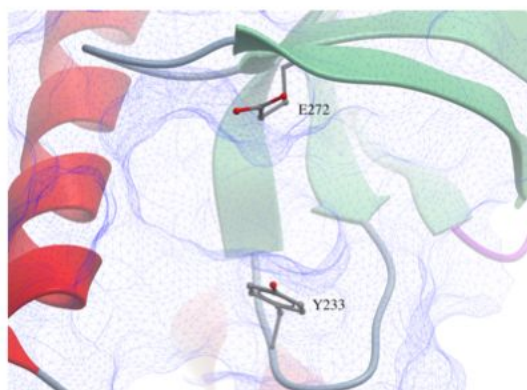
Figure S8. A computational model indicates steric clashes with the isopropyl of compound **3c**. The cyclopropyl of **3f** was replaced with an isopropyl in ICM (Molsoft, San Diego). The isopropyl methyl groups are more distant resulting in increased bulk (the isopropyl geometry is absolutely similar to the one found in ligand bk1, PDB code 3I7B). The energy of the modified flexible ligand was locally minimized in the internal coordinate space, while conserved atoms were tethered to their original position (with a tether weight $tzWeight=200$). The Van der Waals energy of the bound ligand was calculated in ICM (force-field: protein: ECEPP/3, ligand: mmff).



(a)



(b)



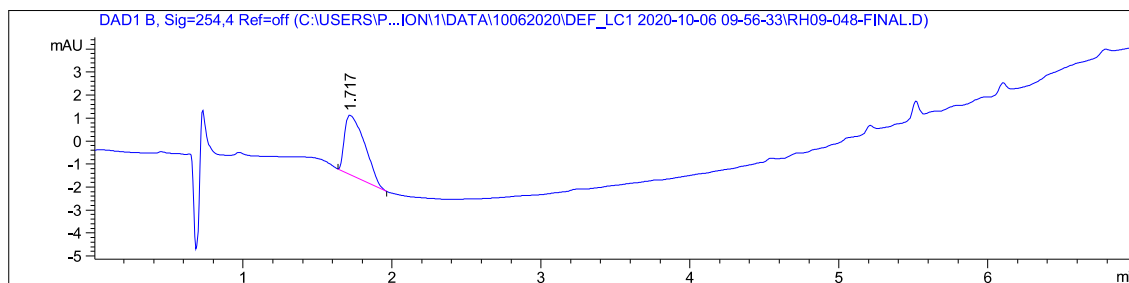
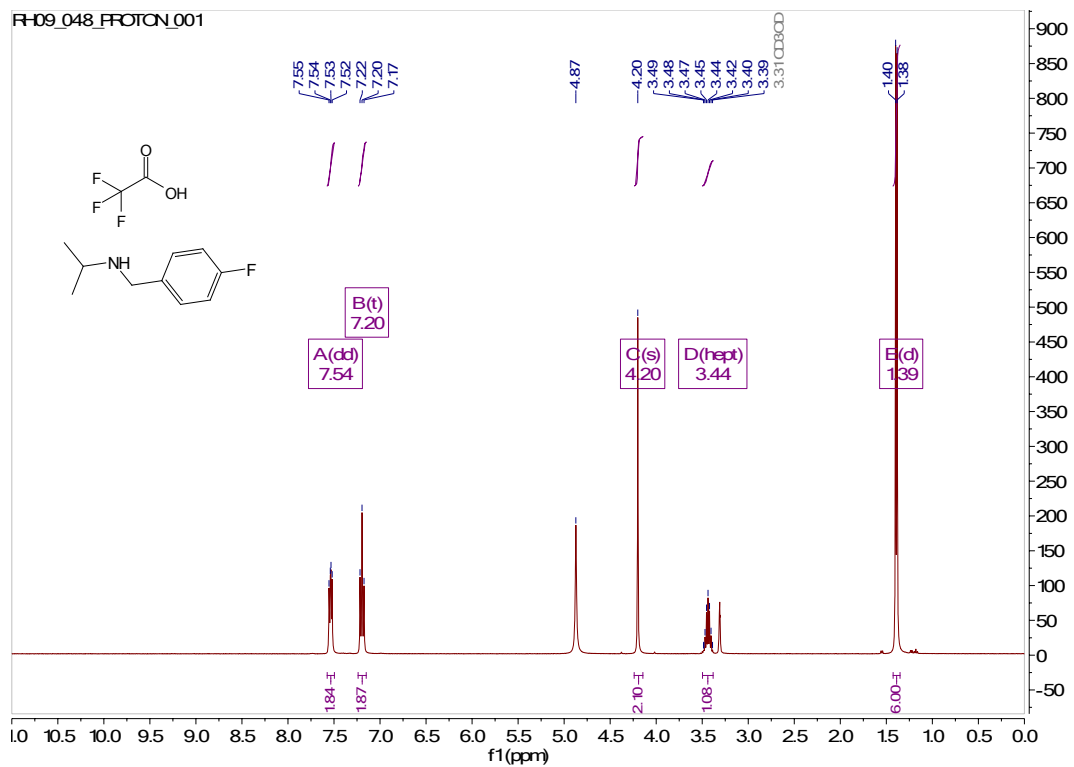
(c)

Figure S9. (a) Comparison between the apo (PDB ID: 5VC8, magenta) and bound (green) conformation of the NSD2-PWWP1. The loop residues G268, D269, A270, and P271 connecting the $\beta 3$ and $\beta 4$ strands

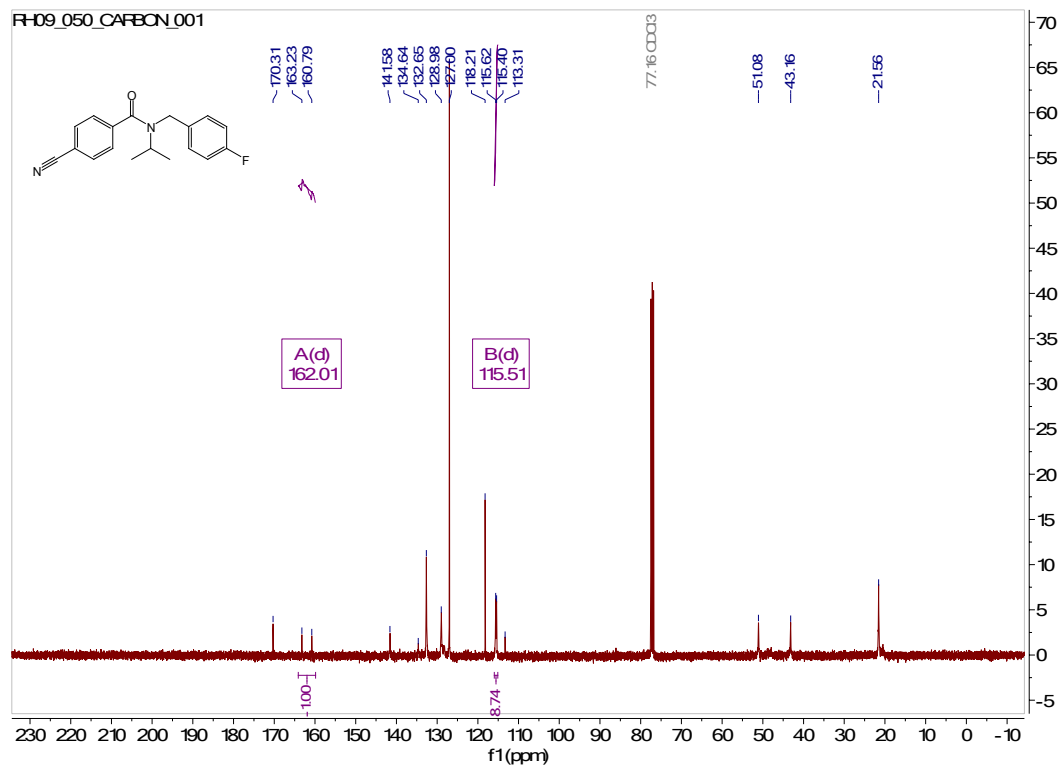
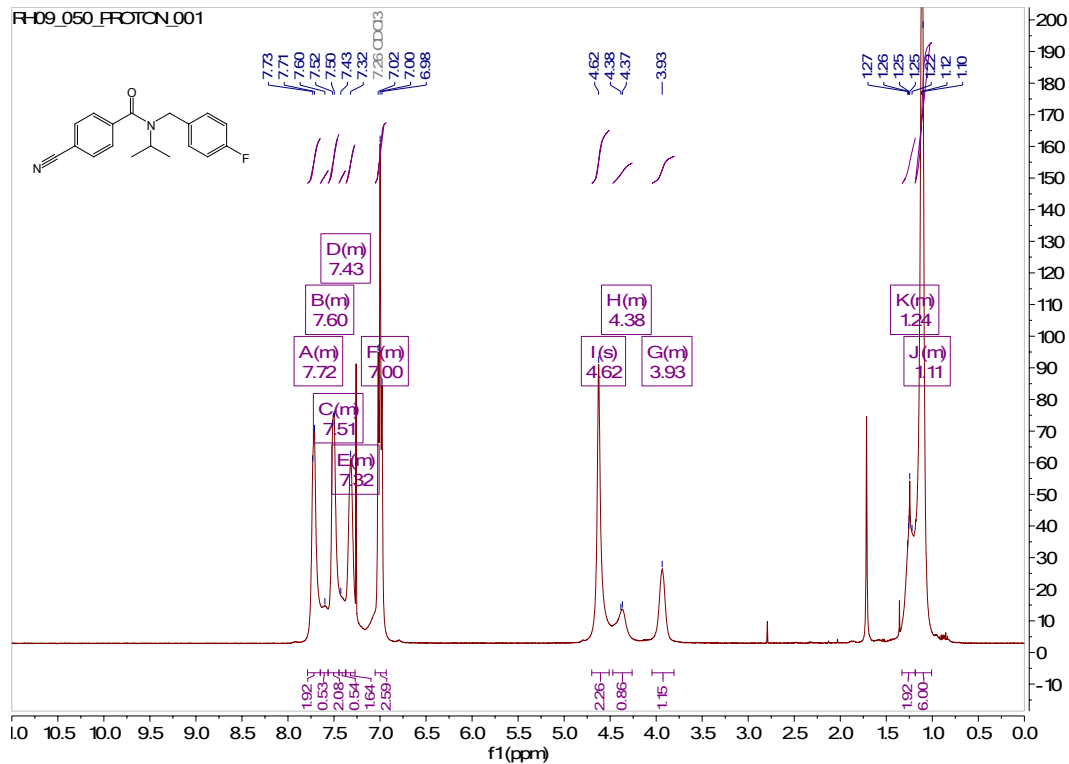
display different conformations in the two structures. (b) In the apo structure the residues E272 and Y233 are closing the pocket. (c) When the ligand binds these residues move away opening the pocket.

¹H NMR Spectra

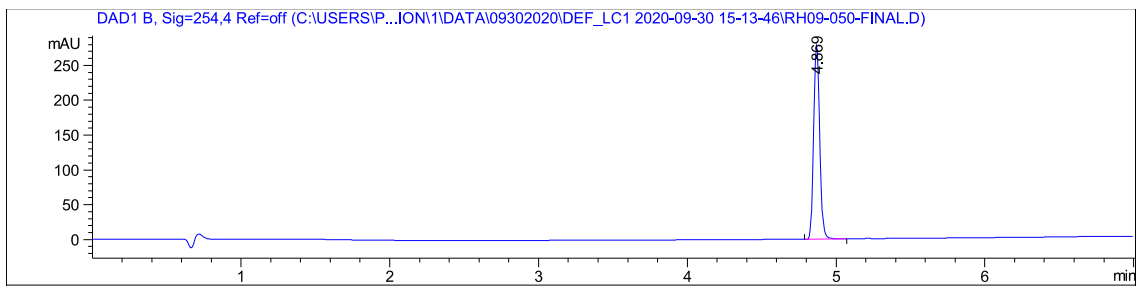
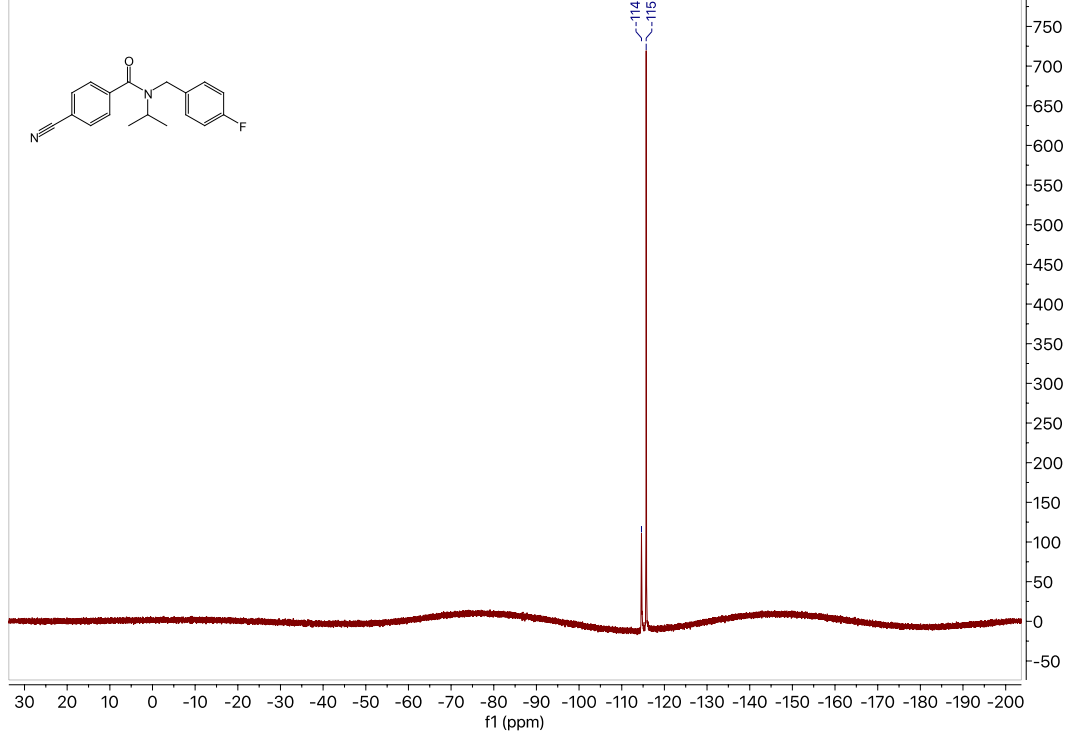
N-isopropyl-4-fluorobenzylamine



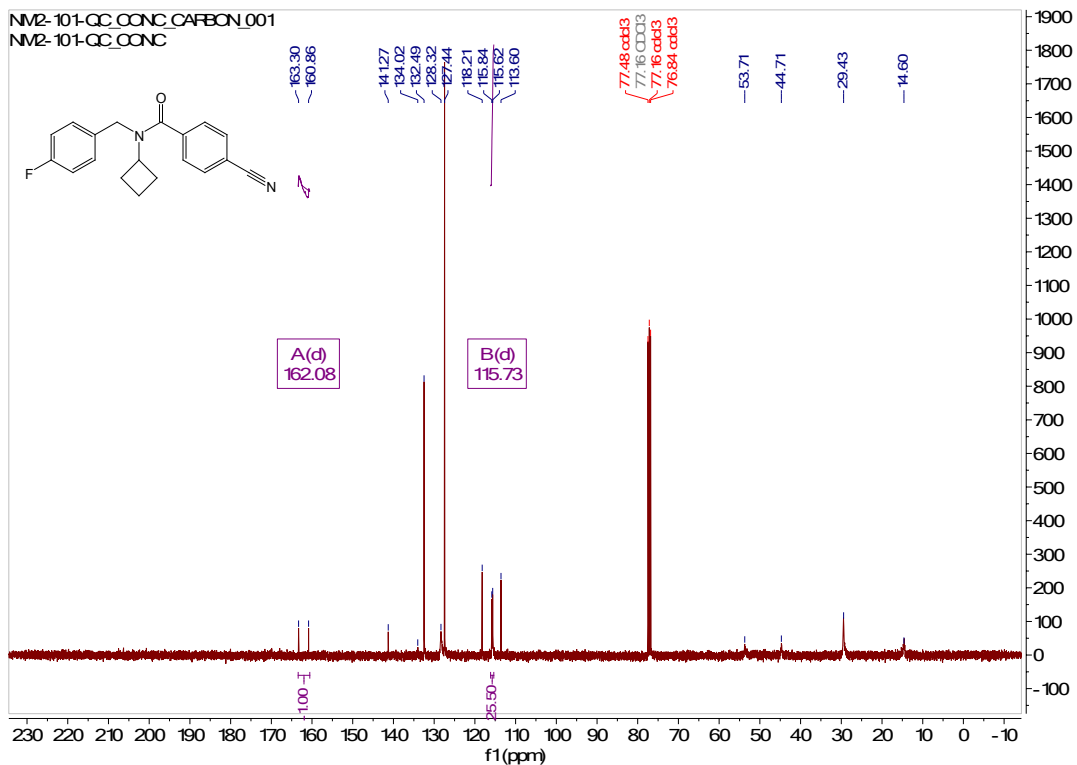
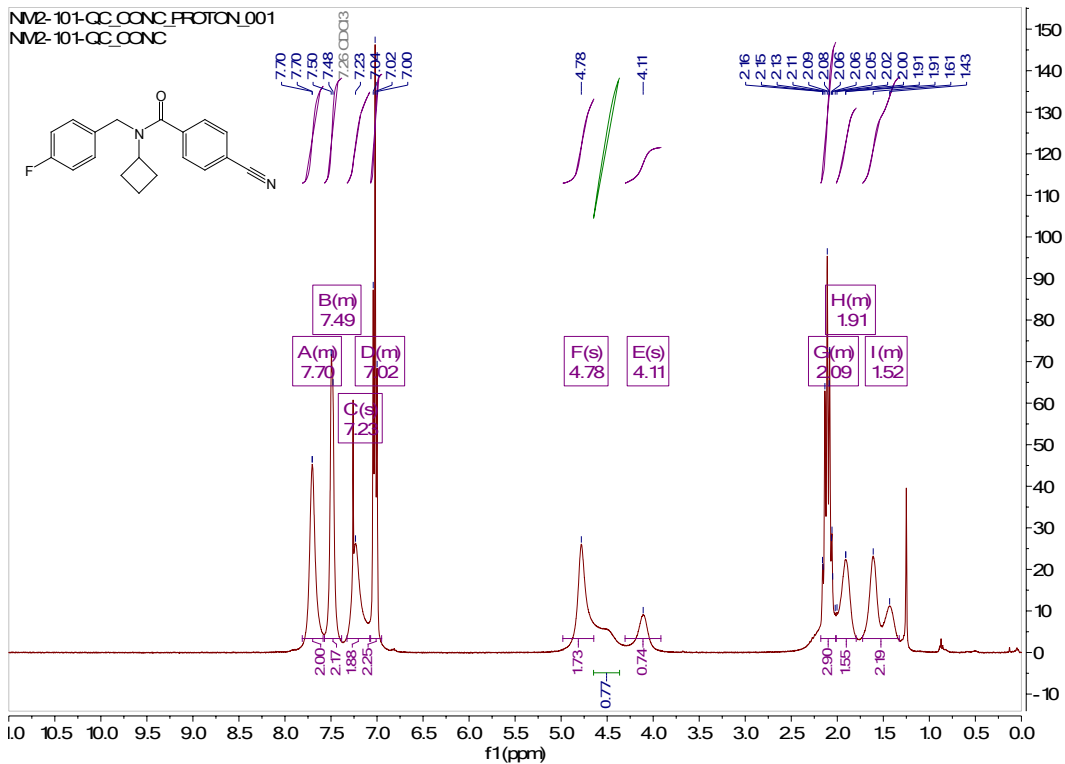
Compound 3c



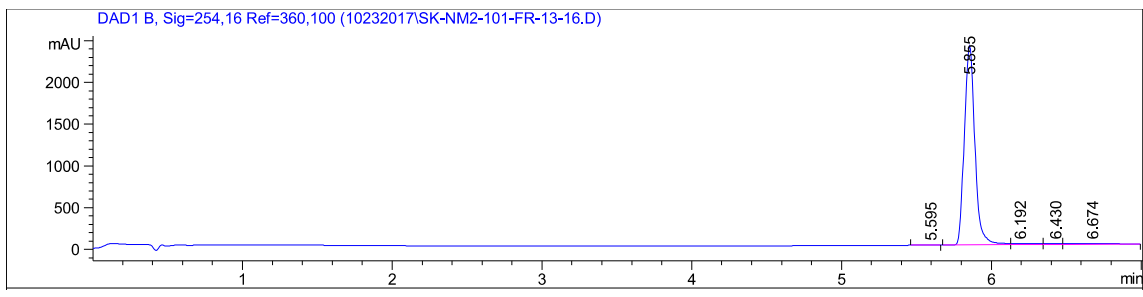
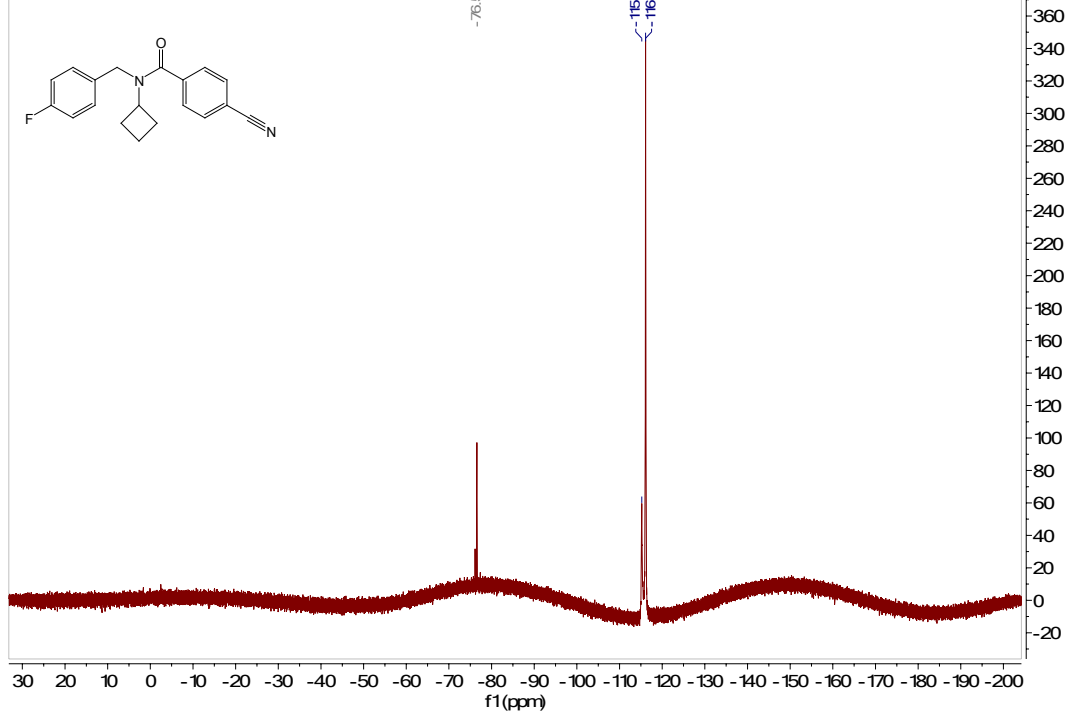
RH09_050_FLUORINE_001



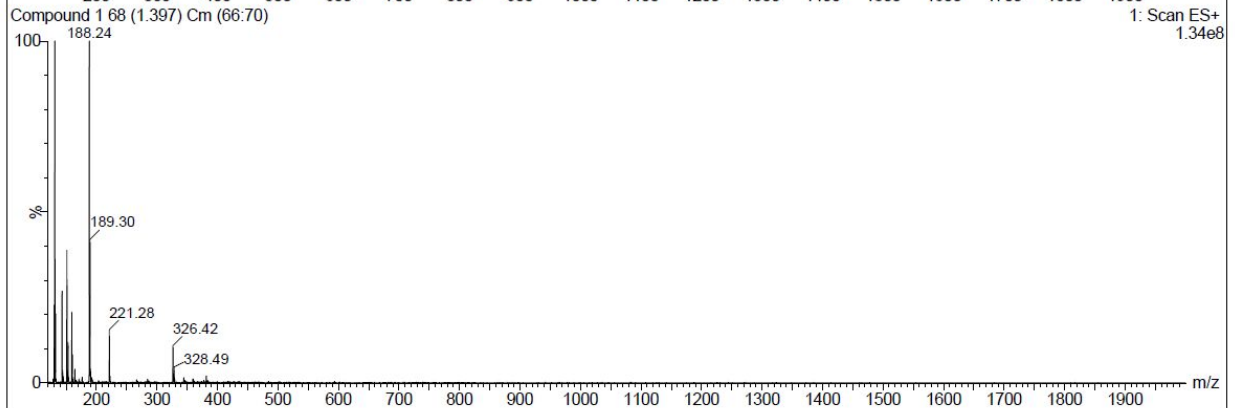
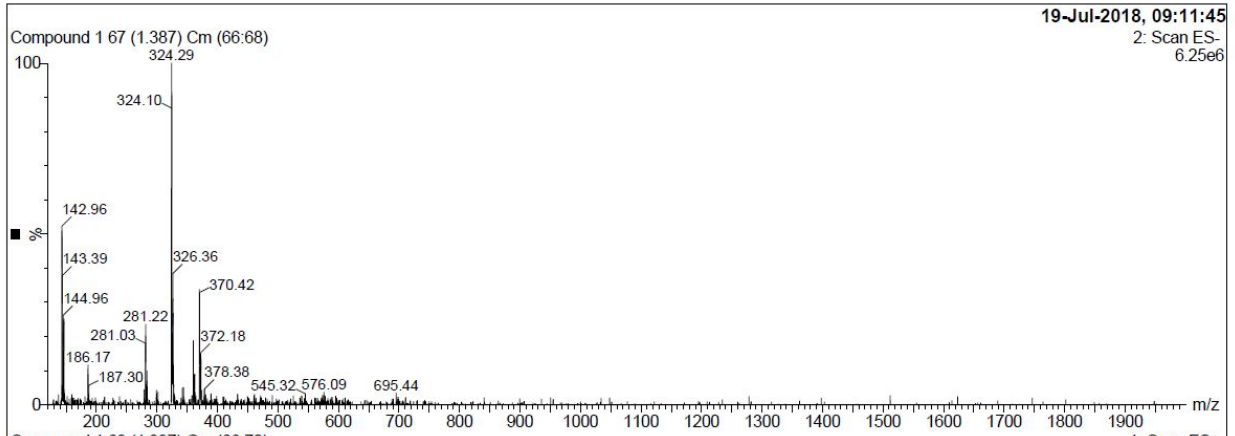
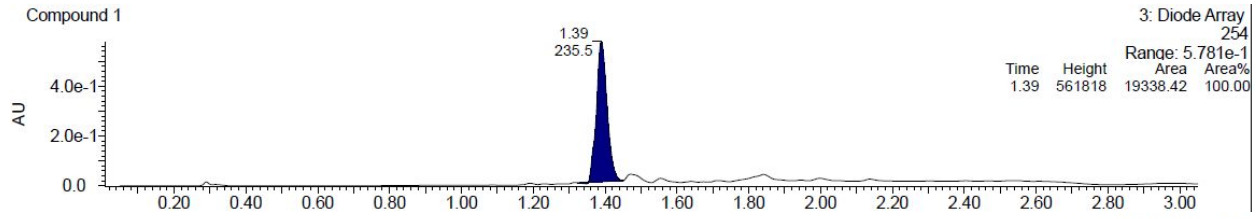
Compound 3d



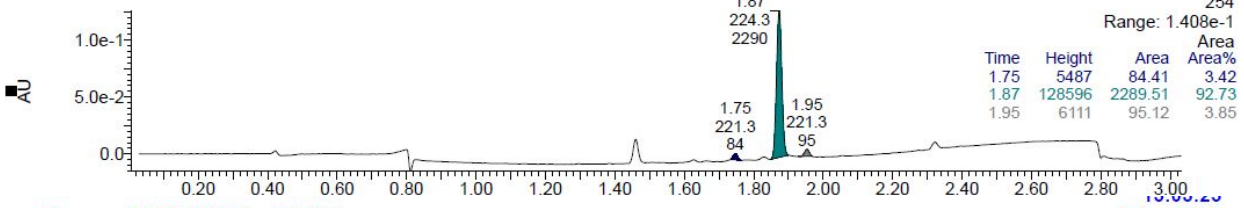
NM2-101-QC.CCNC.FLUCRINE_001
NM2-101-QC.CCNC



Compound purity: analytical spectra

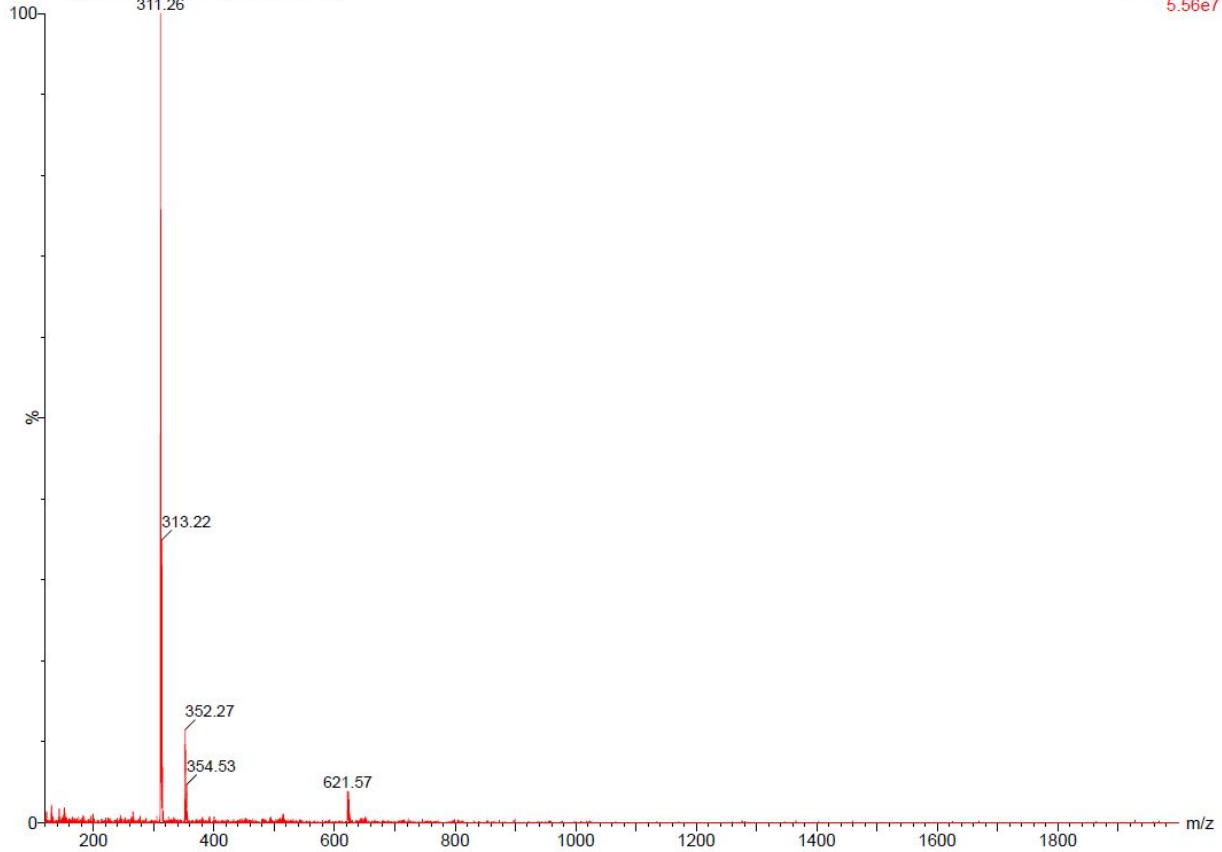


Compound 2

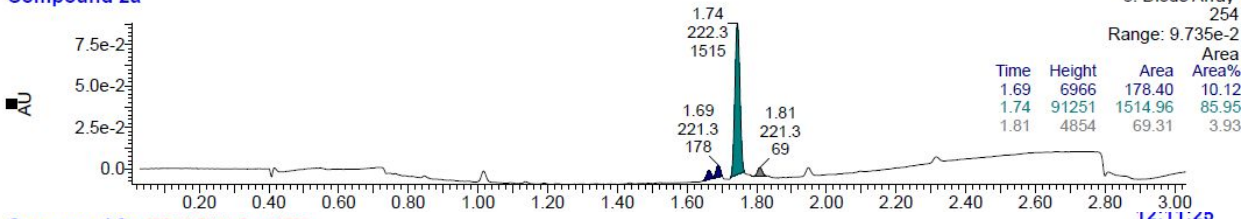


Compound 2 107 (1.863) Cm (107:108)

2: Scan ES+
5.56e7

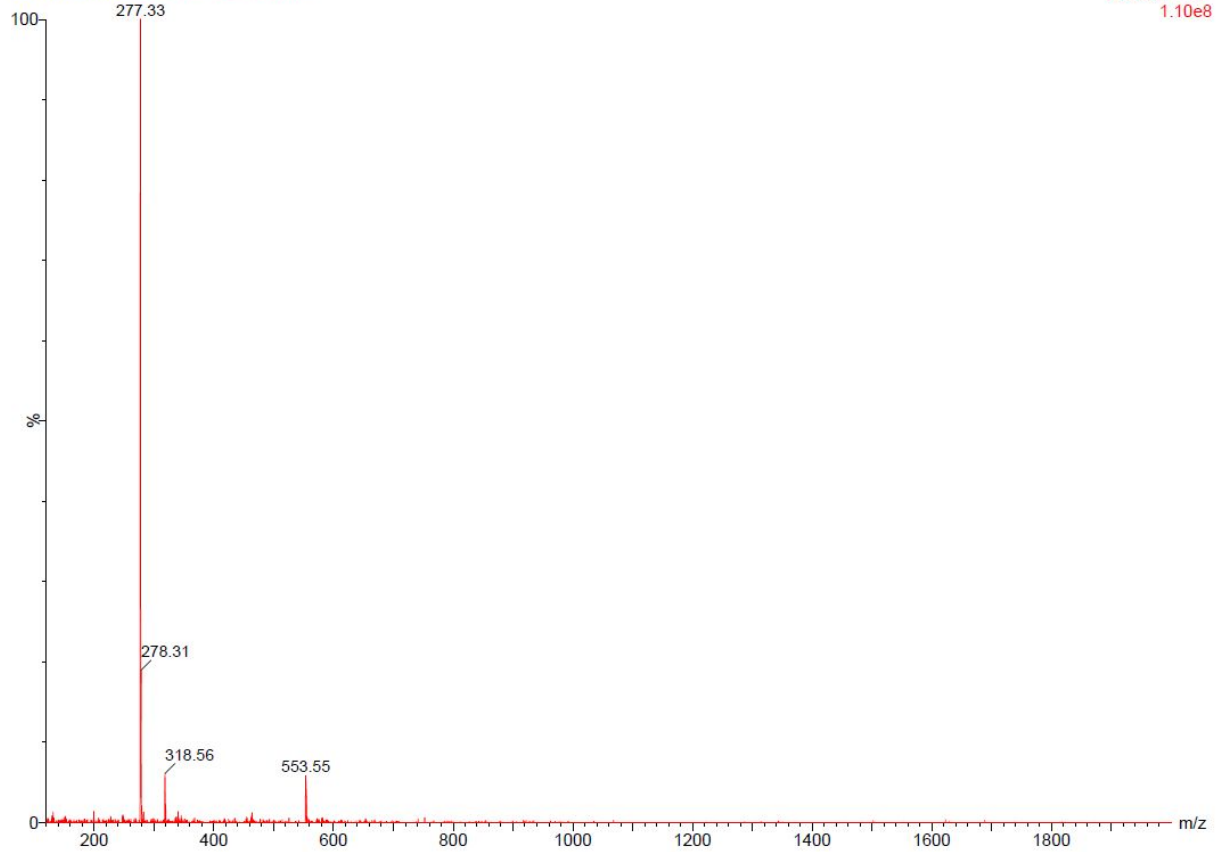


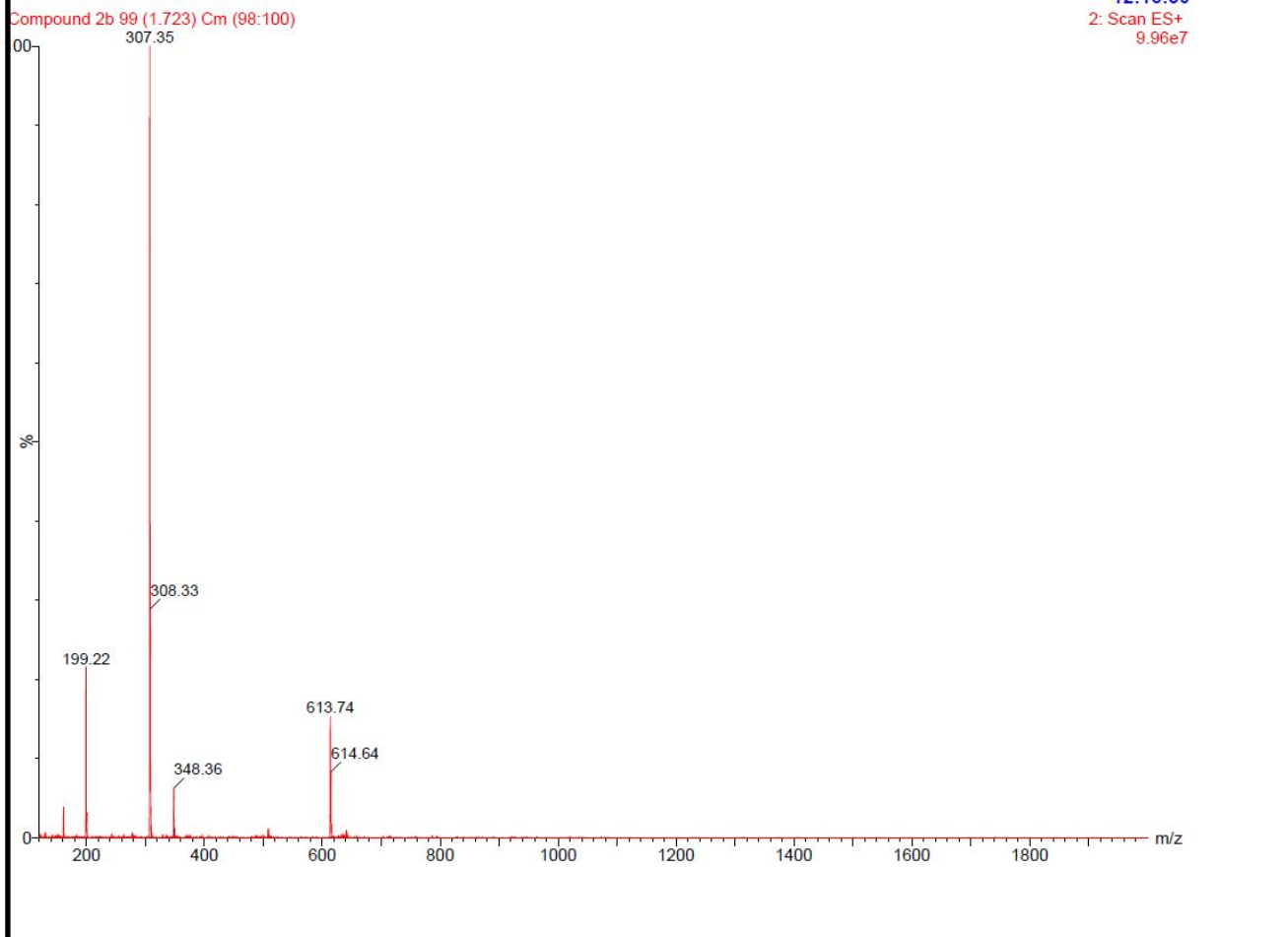
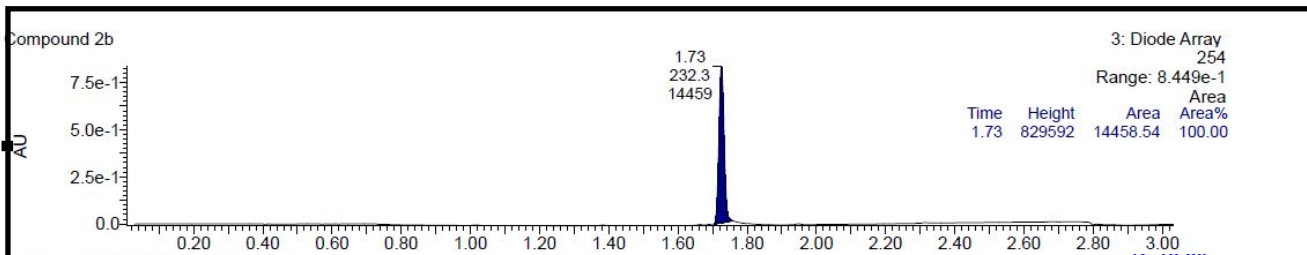
Compound 2a



Compound 2a 100 (1.741) Cm (100)

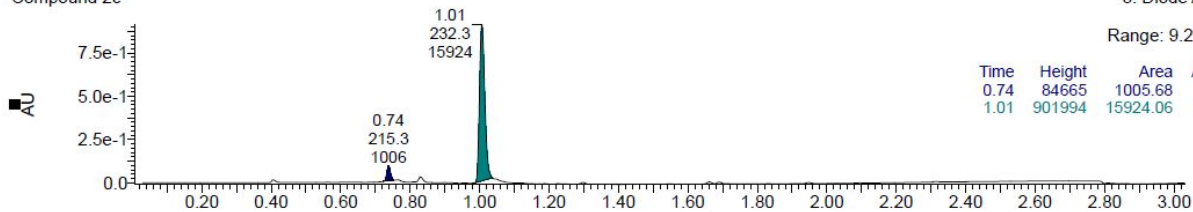
12:11:20
2: Scan ES+
1.10e8





Compound 2c

3: Diode Array
254
Range: 9.228e-1

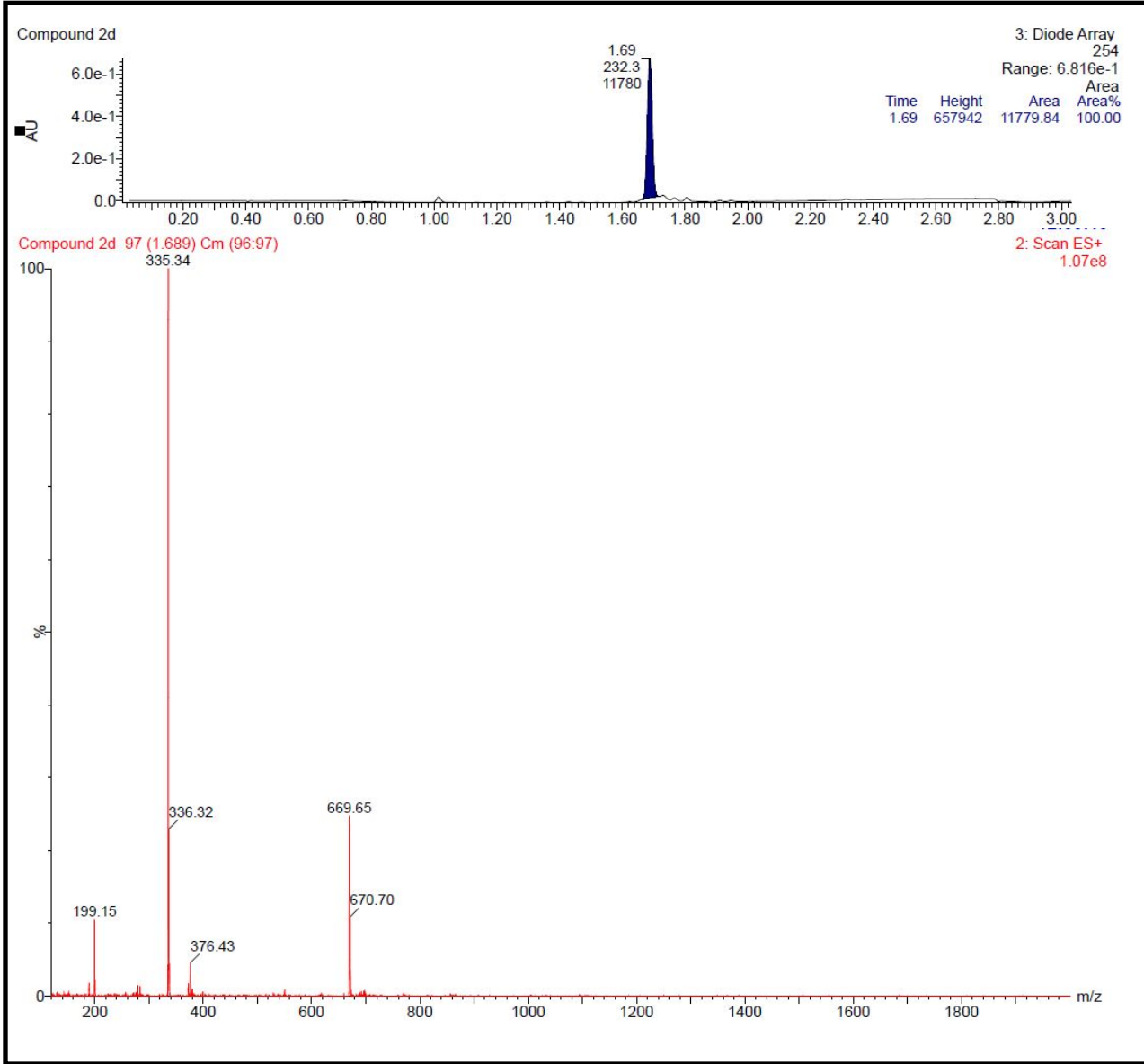


Time	Height	Area	Area%
0.74	84665	1005.68	5.94
1.01	901994	15924.06	94.06

Compound 2c: 58 (1.010) Cm (57:59)

2: Scan ES+
1.21e8

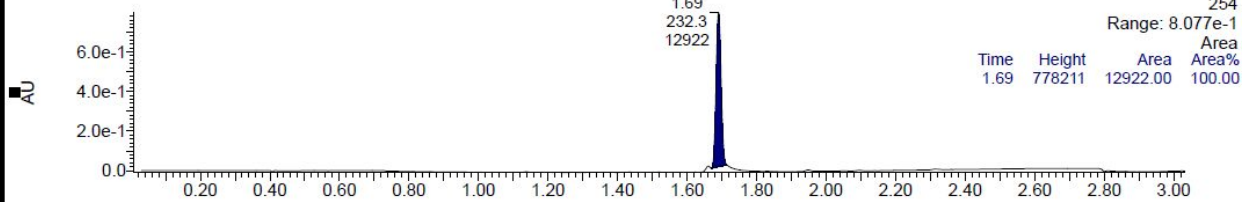




Compound 2e

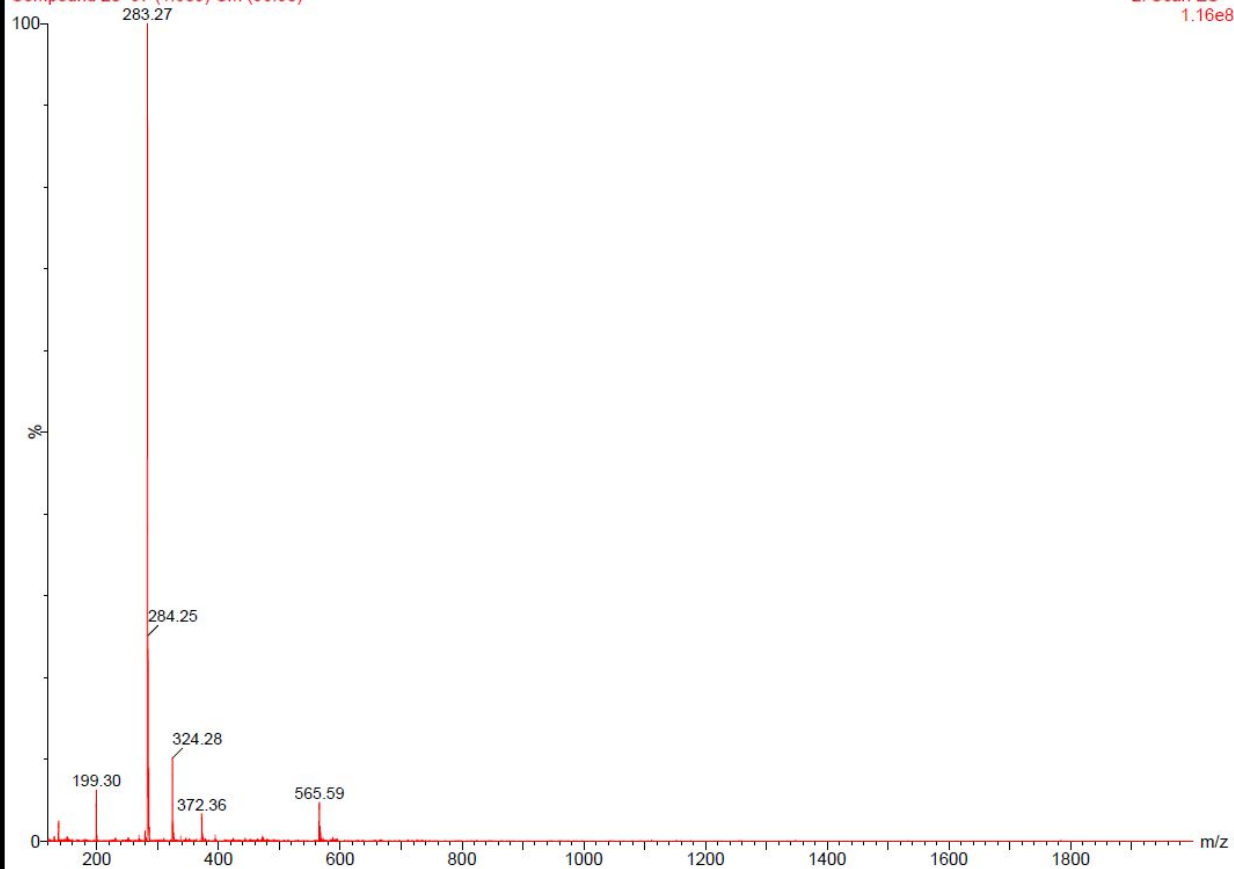
3: Diode Array
254

Range: 8.077e-1



Compound 2e 97 (1.689) Cm (96:98)

2: Scan ES+
1.16e8



Compound 2f

3: Diode Array

254

Range: 1.435

Area

Area%

Time	Height	Area	Area%
1.82	1412134	25345.59	100.00

AU

1.0

5.0e-1

0.0

0.20 0.40 0.60 0.80 1.00 1.20 1.40 1.60 1.80 2.00 2.20 2.40 2.60 2.80 3.00

Compound 2f 104 (1.811) Cm (104:105)

2: Scan ES+

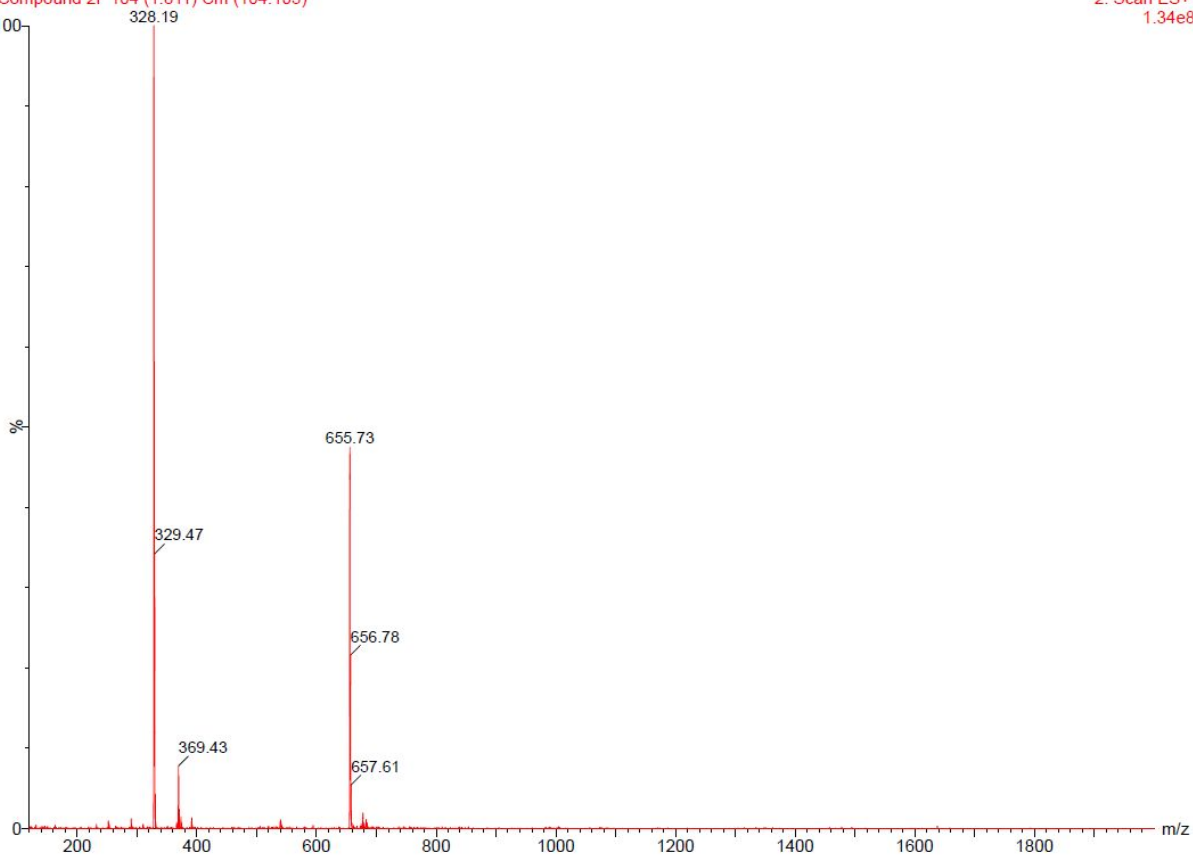
1.34e8

100

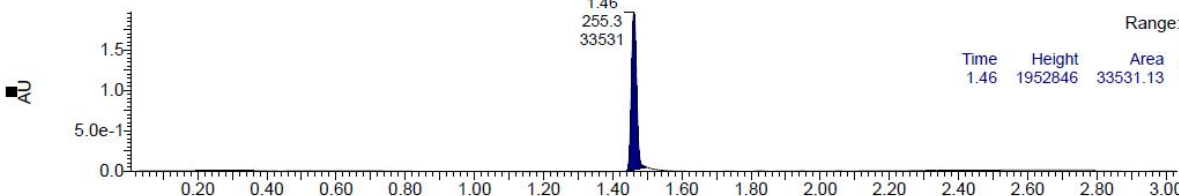
%

0

200 400 600 800 1000 1200 1400 1600 1800 m/z



Compound 2g

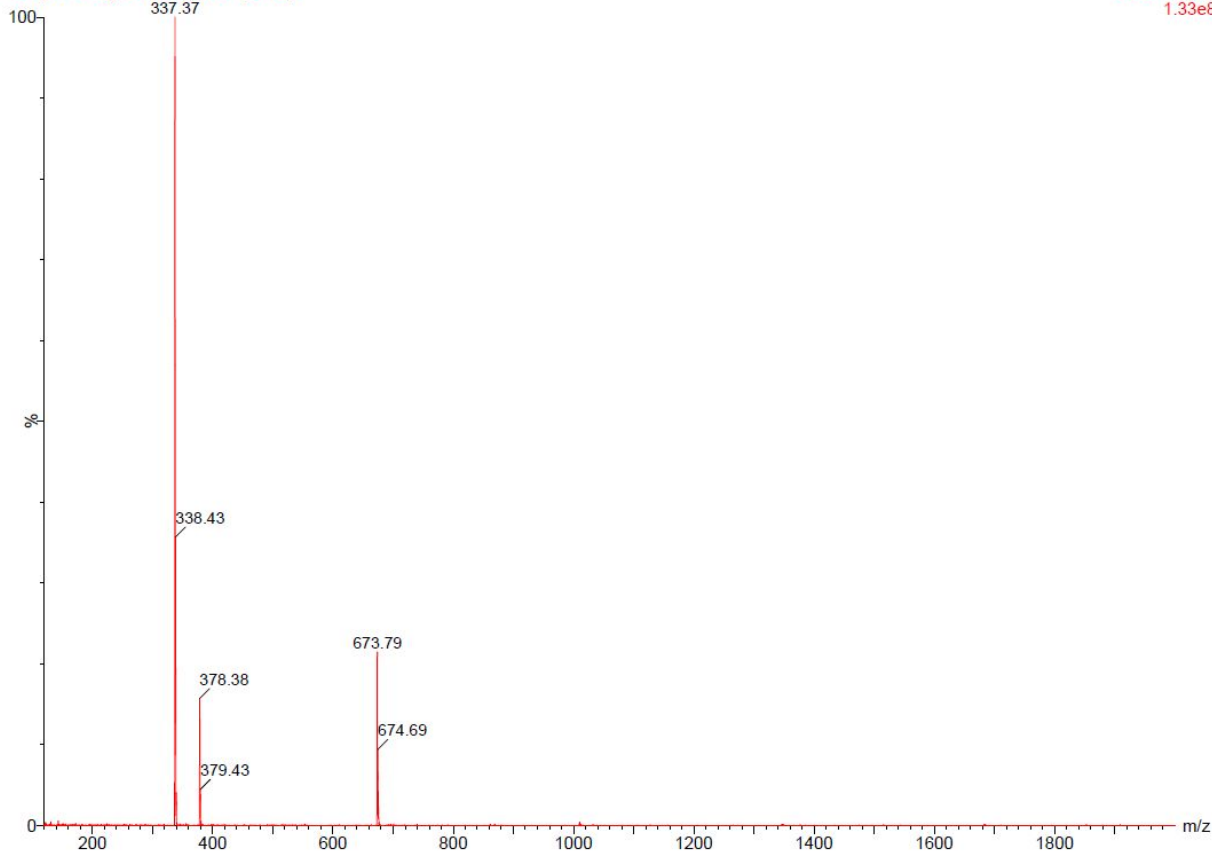


3: Diode Array
254
Range: 1.978

Time	Height	Area	Area%
1.46	1952846	33531.13	100.00

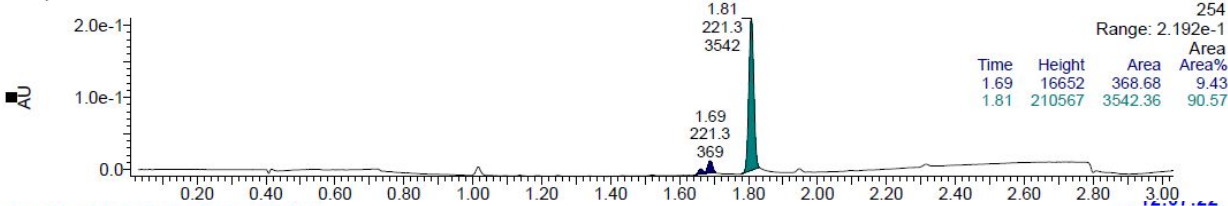
Compound 2g 84 (1.463) Cm (83:85)

2: Scan ES+
1.33e8



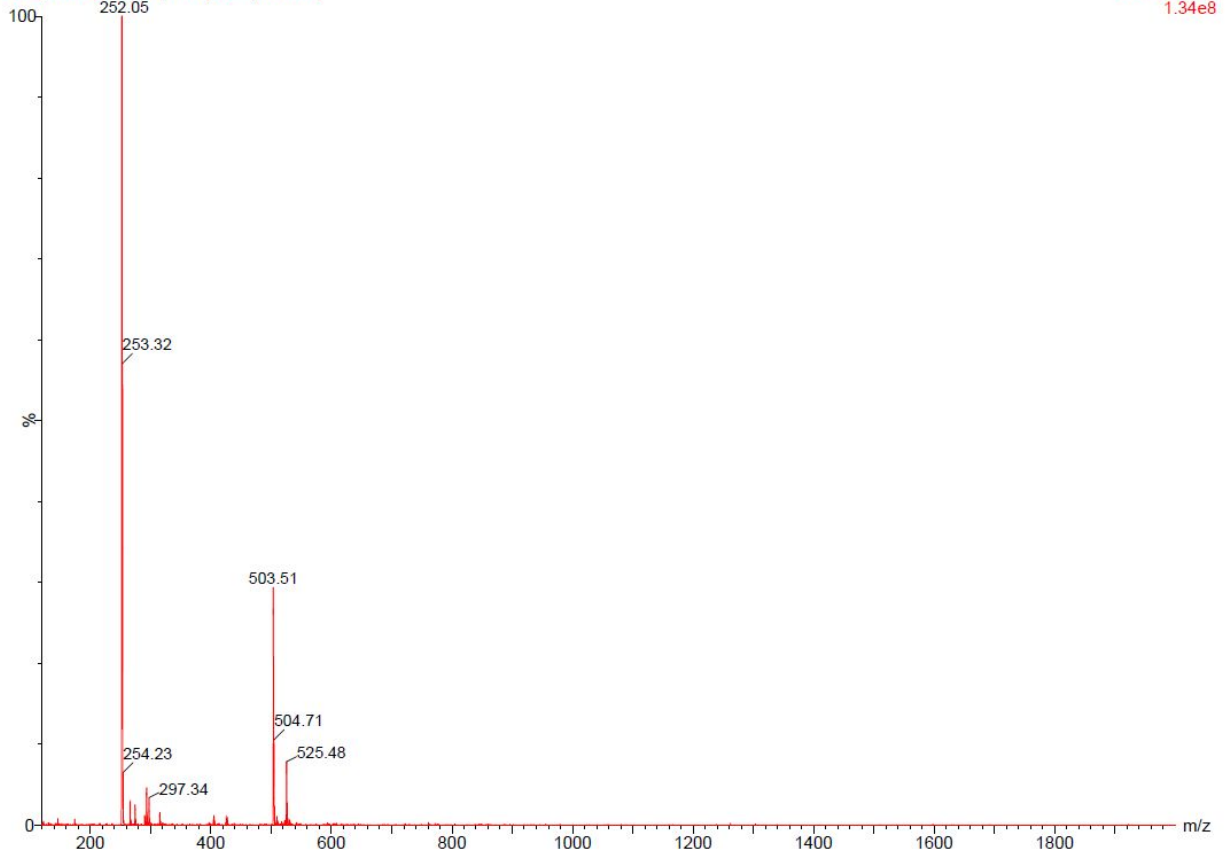
Compound 2h

3: Diode Array



Compound 2h 103 (1.793) Cm (103:104)

2: Scan ES+



Compound 2i

3: Diode Array

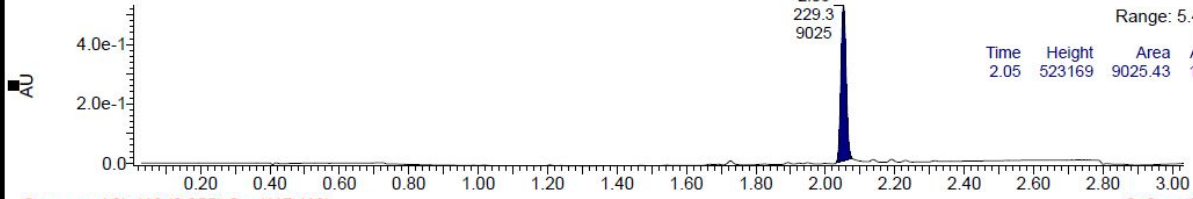
254

Range: 5.41e-1

Area

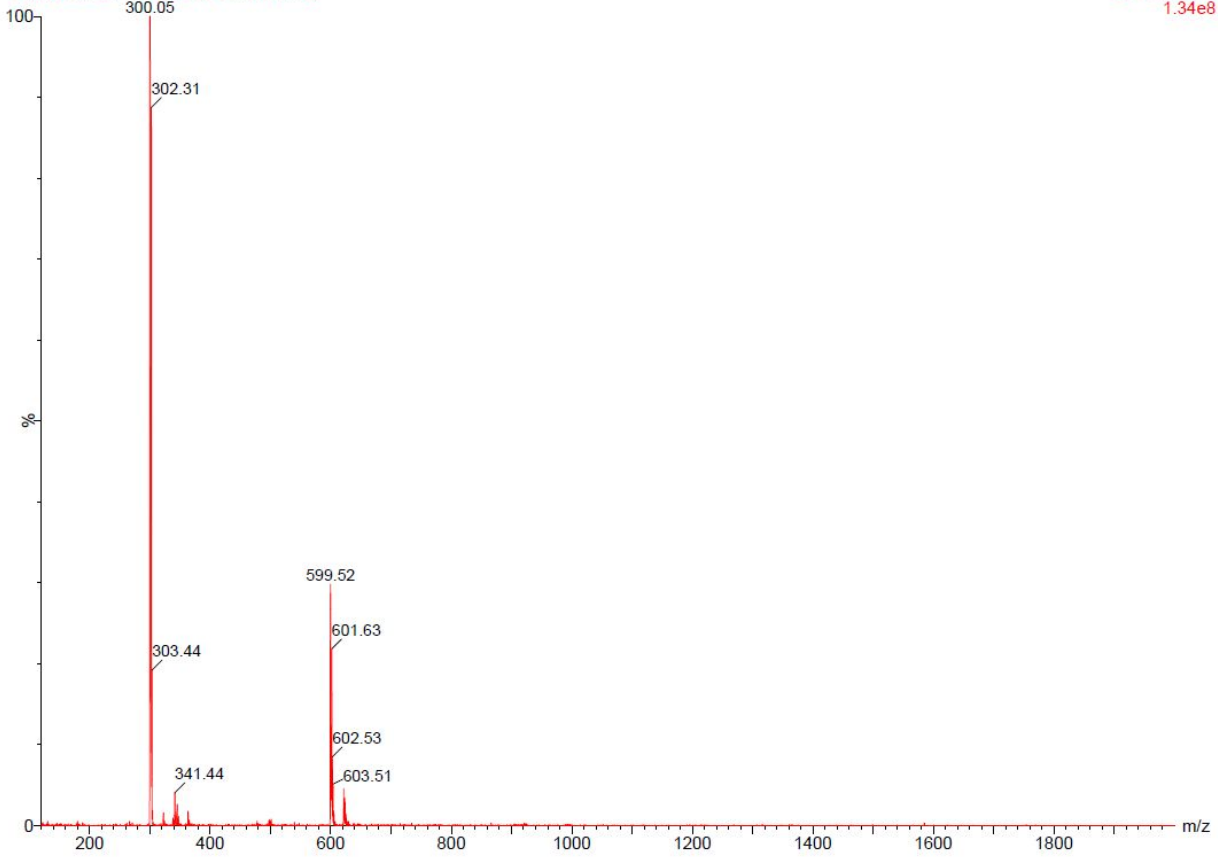
Area%

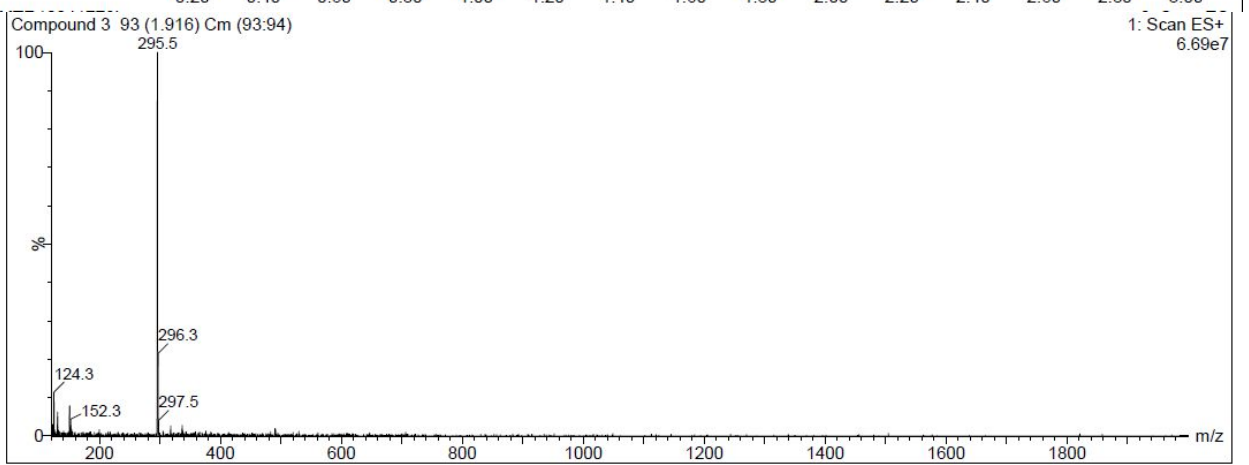
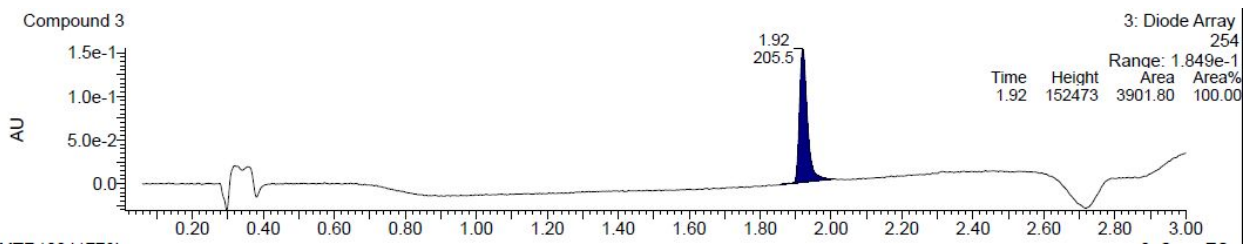
Time	Height	Area	Area%
2.05	523169	9025.43	100.00



Compound 2i 118 (2.055) Cm (117:118)

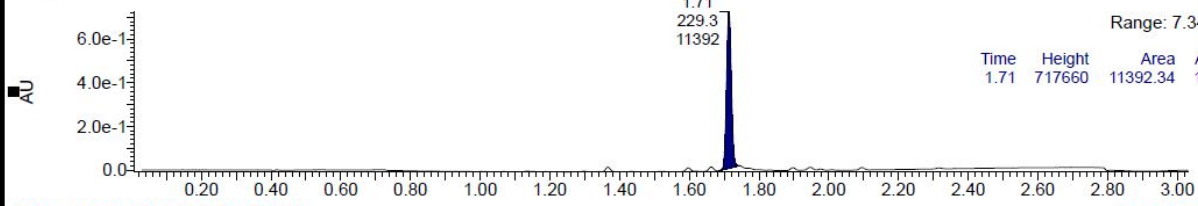
2: Scan ES+
1.34e8





Compound 3a

3: Diode Array
254
Range: 7.344e-1



Time	Height	Area	Area%
1.71	717660	11392.34	100.00

Compound 3a 98 (1.706) Cm (98:99)

2: Scan ES+
1.13e8

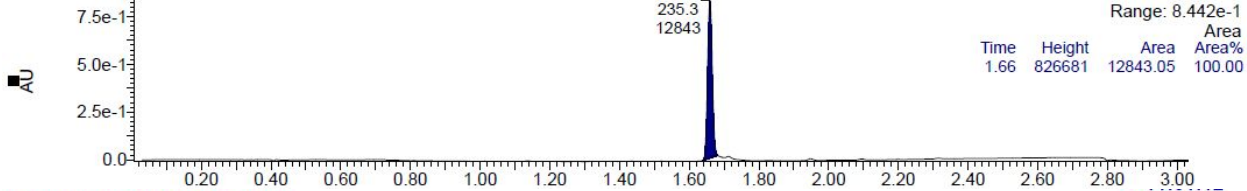


Compound 3b

3: Diode Array

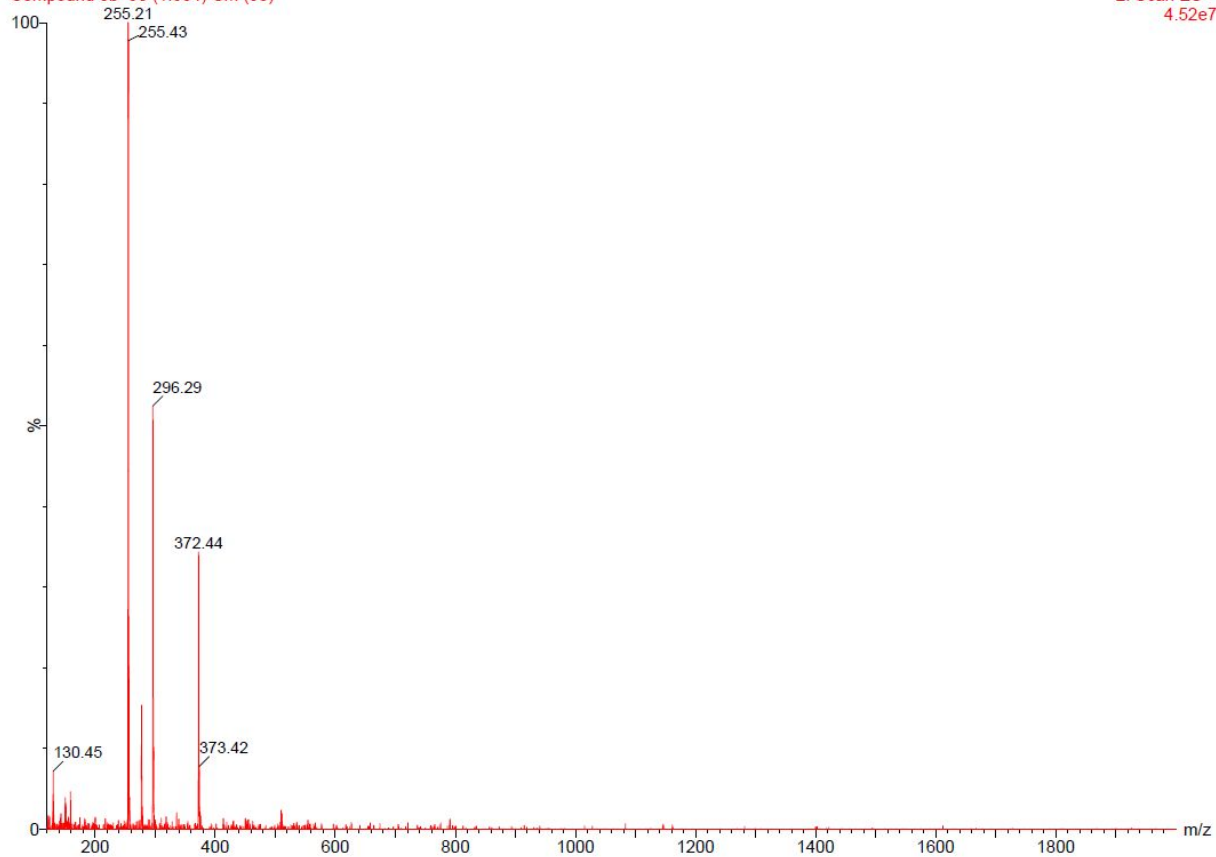
254

Range: 8.442e-1

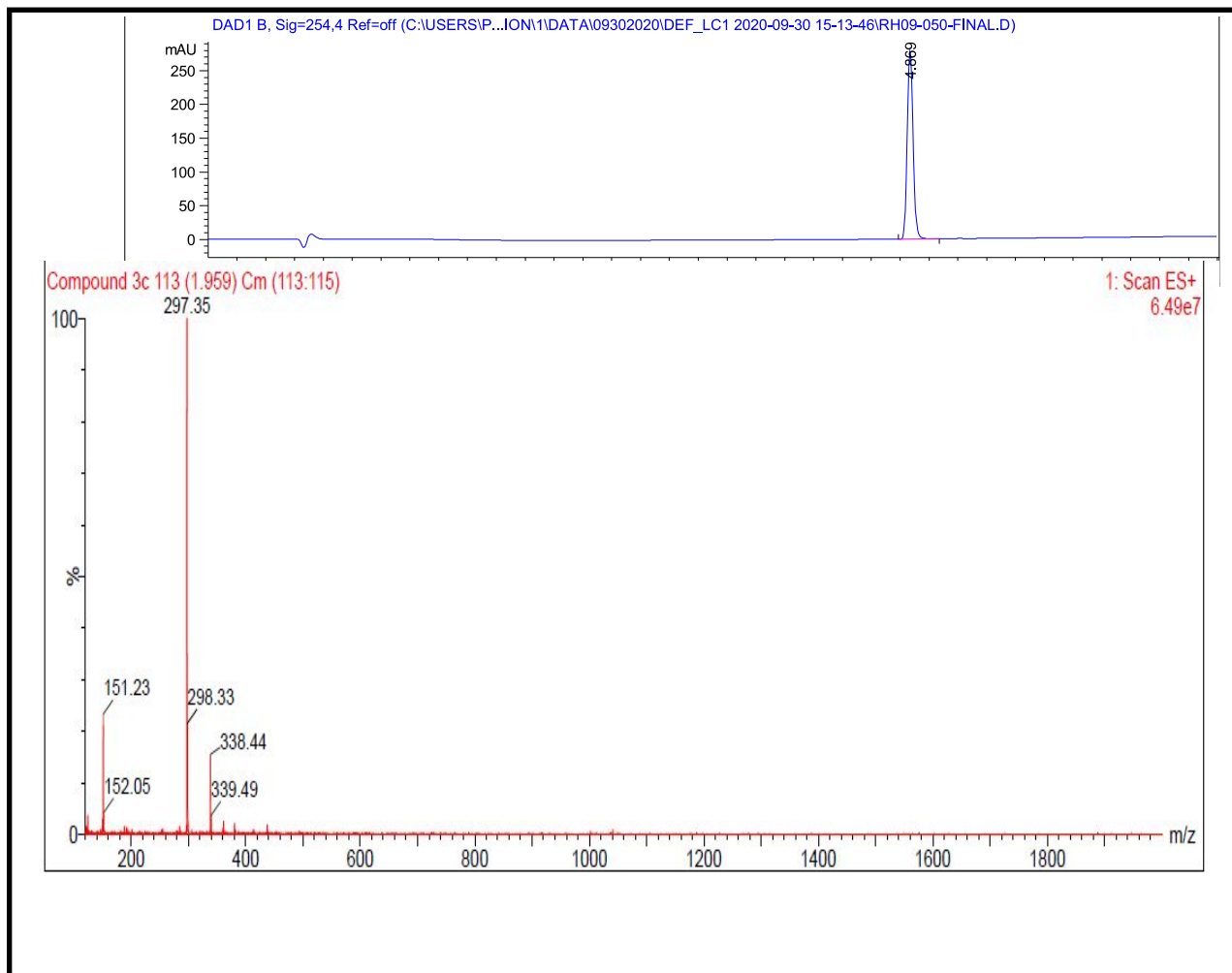


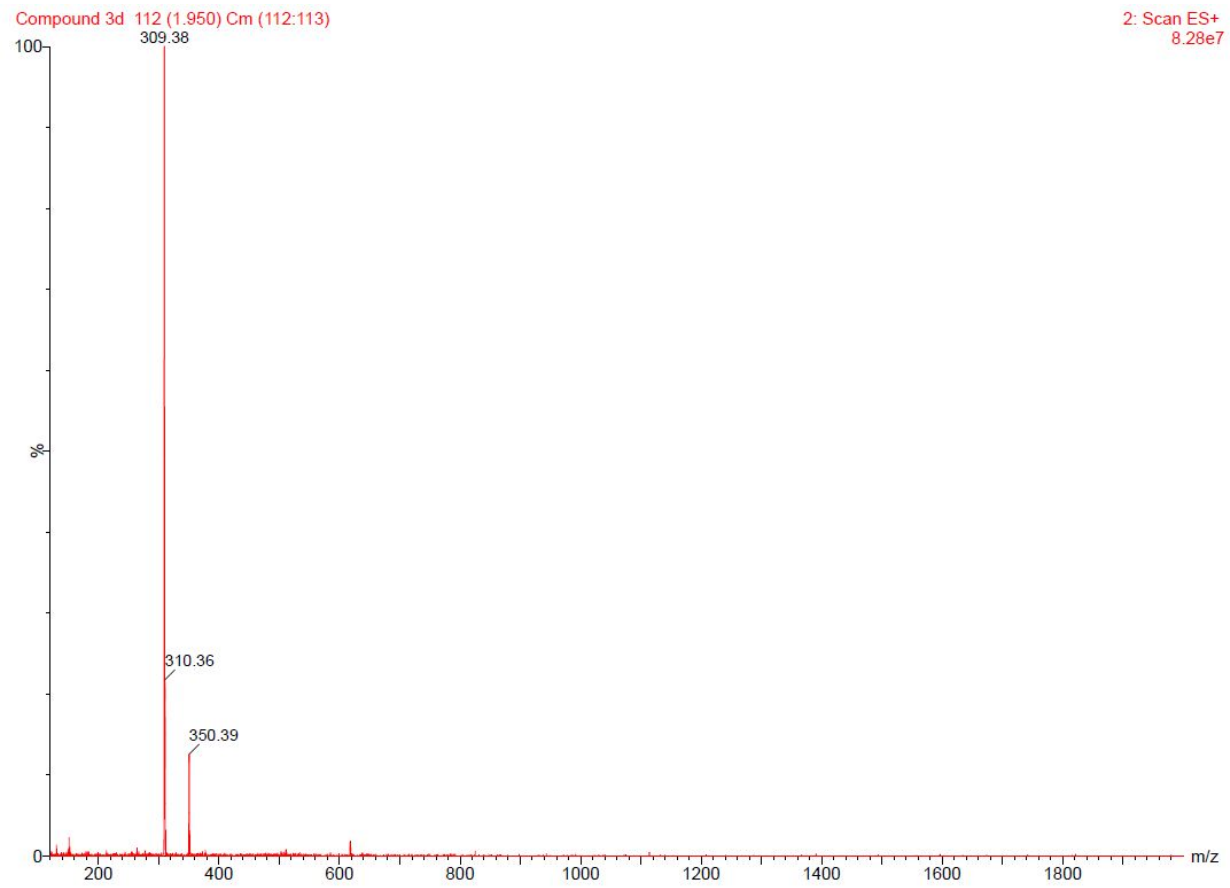
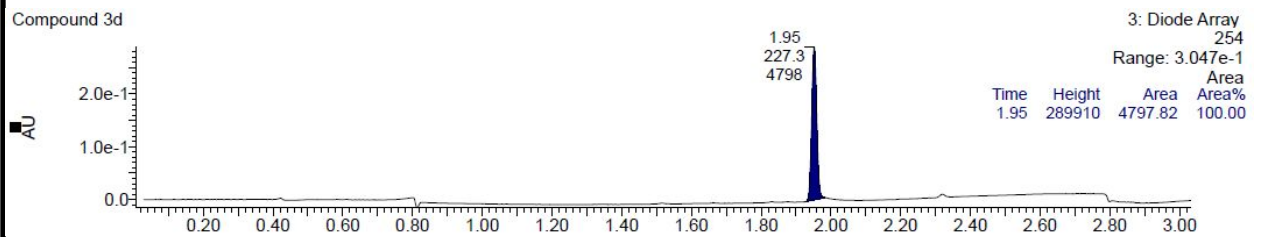
Compound 3b 95 (1.654) Cm (95)

2: Scan ES+
4.52e7

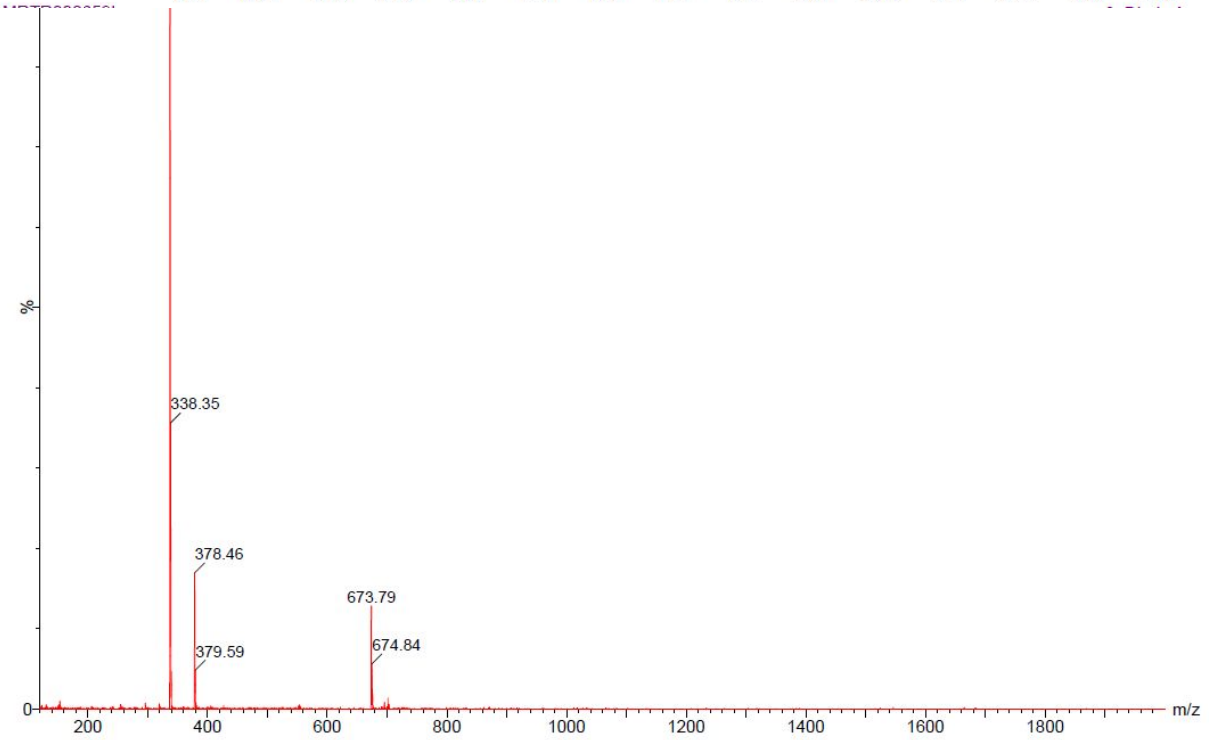
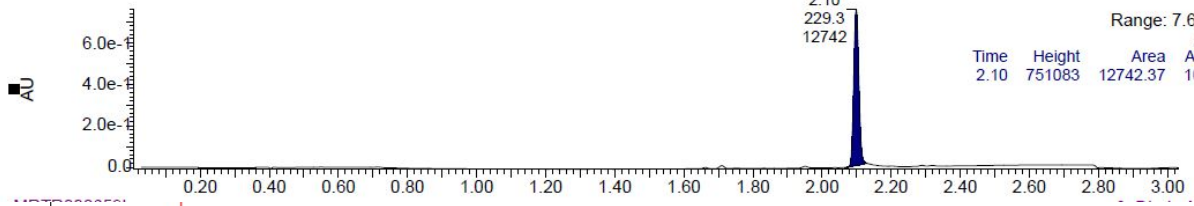


Compound 3c



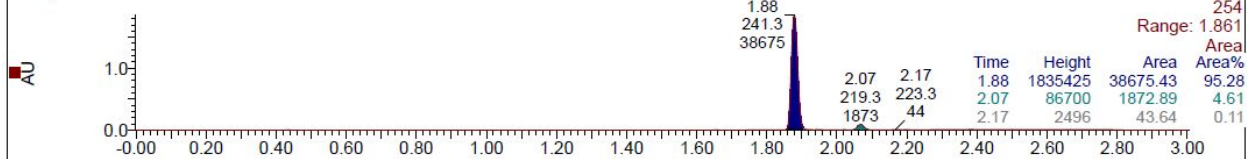


Compound 3e



Compound 3f

3: Diode Array
254
Range: 1.861



Compound 3f_1 110 (1.907) Cm (110:111)

1: Scan ES+
1.15e8

